SSCL Preprint -15

STABILIZATION OF GLOBAL BEAM CONTROL FEEDBACK LOOPS FOR SSC LOW ENERGY BOOSTER USING SLIDING-MODE CONTROLLERS

L. K. Mestha
SSC Laboratory*, Dallas, Texas 75237

C.M. Kwan and K.S. Yeung
University of Texas, Arlington, Texas 76019

Abstract

The accelerating frequency of the Low Energy Booster planned at the Superconducting Super Collider Laboratory is designed to vary between 47MHz to 60MHz in 50ms. Such a large variation in frequency places greater demands on the global beam control feedback loops. A new method of synchronizing the Low Energy Booster with the Medium Energy Booster is under development. This type of approach demands a high level of stability analysis of the feedback loops since it interacts with other loops already in operation. In currently operating machines, classical feedback controllers are used. In the presence of non-linearities, field errors and measurement errors, the classical controllers fail to give good control over the synchronization. Sliding-mode controllers can give robustness to the loop in the presence of uncertainties. However, it requires the knowledge of beam model with some indication of the uncertainities and non-linearities. Therefore, in this paper we show a brief description about the derivation of the control model and then the design of two types of sliding-mode controllers. The first sliding-mode controller is conventional and the second is designed by input-state linearization of the original non-linear equation. The simulation results show that the loop performance is good in the presence of errors compared to the linear state feedback controllers.

1. Introduction

There are two important parameters such as the magnetic field and the accelerating voltage associated with the beam control. Since the magnetic field system is responsible to bend and focus the beam, it has a long time constant. Hence all the beam control feedback loops are concentrated at the Radio Frequency (RF) accelerating system. There are 8 RF accelerating cavities planned for the Low Energy Booster (LEB), located in one superperiod with necessary geometrical spacing between them as shown in Figure 1. The RF cavities are driven by programmed amplitude and frequency function. RF power amplifier drives the cavity and a high voltage appears on the gap. The amplitude of this voltage is programmed and is controlled by each cavity local feedback loop (Mestha 1991). The frequency function is generated globally to all the cavities.

1.1 Description of the Planned Synchronization Loops

The low power RF signal driving the cavities are generated by a single frequency source, namely a Direct Digital Synthesizer (DDS). The frequency and phase of the RF signal is controlled with feedback loops from the beam to the frequency source and a global phase shifter. The local phase shifters are passive. They are required only to phase the RF signal going to each cavity due to the geometrical spacing between the cavities. By varying the frequency and phase of the RF signal the voltage seen by the beam and hence the energy

***Operated by Universities Research Association Inc., under contract with U.S. Department of Energy, Contract No. DE-AC02-89ER40486**

can be varied.

There are errors in the bending magnetic field which lead to orbital deviation in the form of radial position if the beam energy is not matched to the magnetic field. The deviation in the orbital position is measured with horizontal electrodes of the beam position monitor and is corrected by varying the phase of the RF signal in the global phase shifter. This loop is called the 'radial loop'. This loop has generally slow time response and is not able to damp 'coherent dipole oscillations' in the beam due to field errors. Therefore a 'beam phase loop' is included to the frequency source. In this loop the beam signal is compared directly from a wall current monitor with the RF signal in a beam phase detector. It is compared to the synchronous phase of the beam and an error signal is obtained. The error signal is proportional to the dipole oscillations in the beam. The beam phase error is converted to appropriate frequency shift through a feedback controller. The frequency shift is added to the programmed frequency curve at the input end of the DDS.

With only radial and phase loops the beam will circulate around the ring without proper synchronization of a given bunch with the stable bucket in the Medium Energy Booster (MEB). The synchronization is required for filling batches of LEB bunches into the MEB for collider operation. The configuration of the synchronization loop shown in Figure 1 provides the means to phase-lock the reference beam bunch in the LEB to the reference bucket in the MEB (Mestha, 1991). In this approach a Time to Digital Converter (TDC) is used to measure the position of the designated LEB reference bunch for each MEB revolution. The time of flight information is multiplied with a stored velocity profile for the synchronous particle. By comparing these values with the ideal phase values for the designated LEB reference bunch for each MEB revolution an error signal is generated. The error signal is converted to frequency shift from the controller which is then added to the ideal frequency program. Thus the LEB reference bunch is phase-locked to the ideal phase values stored in the computer. This enables phase-locking of the bunch with controlled phase slippage when ideal phase values are suitably adjusted for transfer.

1.2 Goal of Robust Controllers for the LEB

The feedback strategy described above has been studied with linear state feedback controllers in Reference (Mestha, Kwan, Yeung, 1991) for small operating region. The beam control model is non-linear, time varying and has field error terms as uncertainties. Although the implementation of Figure 1 looks simple, stability and performance of the loops are not guaranteed when there is significant uncertainties and non-linearities. The uncertainties in our control problem are (1) Field errors (Cavity voltage and magnetic field) (2) Errors in the measurement of radial position (3) Systematic and random errors in the beam phase measurement (4) Errors in the frequency source due to the stability limits on oscillators (5) Errors in calculating the 'trip-plan' (6) Errors while ramping the programmed frequency. The linear controllers shown in Figure 1 do not guarantee optimal performance and stability under these conditions. Hence, in this paper we have shown briefly the derivation of the non-linear beam model associated with the control objective and then, we introduce the design of two sliding-mode controllers to overcome the effects of errors mentioned above. The implementation of such a scheme does not look far from reality not only due to the advancement in the technology of Direct Digital Synthesizers and the computational power of Digital Signal Processors, but is also due to the simplicity in modifying the planned hardware (with state feedback controllers of Figure 1) to add the robustness offered by the sliding-mode controllers.

The first sliding-mode controller is conventional and is designed to minimize the linear combination of the synchronization phase error, beam phase error and the radial position error to zero. Whereas with the second controller, the objective is targeted towards achieving the synchronization phase error zero at all time after reaching sliding. It is applied to the beam model after input-state linearization to achieve robustness to the loop. The input-state linearization techniques hitherto are used to only autonomous systems and they are not robust. With the application of sliding-mode techniques, a generalized design shown in this paper can handle the non-autonomous case in the presence of uncertainties.

2. Beam Control Model

For the purpose of designing feedback control law to operate in the presence of errors and system non-linearities, a good tracking model is helpful. We can derive the model by using a macro-particle concept, in which a single particle is tracked turn by turn and rest of the particles in a bunch are assumed to follow the single particle. A beam bunch in this paper is referred to as a macro particle. The longitudinal dynamics contained in the turn by turn tracking model is then transformed to the differential equation form by identifying suitable control inputs. Detailed description of the derivation of the model is covered in Reference (Mestha, Kwan, Yeung, 1991).

For describing the tracking of a single macro particle we will consider the circular orbit in the LEB. Whatever the shape of the real orbit of the particle, its shape is replaced by circle with circumference equal to the actual path length as shown in Figure 2. For mathematical consideration let us consider a simple case with a single accelerating cavity with an infinitesimally small gap length inserted in the beam line as shown in this Figure. The particle travelling in the beam line will see accelerating field only at the pointlike gap and will see no accelerating field elsewhere. Analogous to the accelerating case we also consider thin magnetic lenses such that the magnetic field will be maintained constant for one complete traversal across the gap. The magnetic field will be changed each time at the exit from the gap along the particle orbit.

As we pointed out in Figure 1, our ultimate goal is to be able to synchronize a given beam bunch from the LEB with a selected reference bucket in the MEB without loosing particles and diluting emittance. The LEB has 114 bunches and the MEB has 792 stable buckets and some of them may be filled. While synchronizing, we must make sure that the orbital deviation is under control and the beam phase oscillations are damped. In this paper, we will show briefly the derivation of specific equations representing the system dynamics useful for designing sliding-mode controllers. First we obtain the synchronization model in terms of the machine parameters and then show the derivation of the model for orbital deviation and the phase oscillations.

2.1 Synchronization Model

As indicated above, in the synchronization loop the reference particle of the LEB is tracked with respect to a designated stable bucket of the MEB. Let $\tilde{t}_k^i$ be the time covered by the ideal reference bucket in the MEB for kth turn in the LEB. If t_k^i is the time when the reference particle in the LEB reaches the reference point in the kth turn, then if v_k^s is the velocity of the reference particle, the 'trip-plan' is given by:

We have plotted the trip-plan for the LEB to MEB synchronization in Figure 3. The values

$$(\psi_k)_{Trip-plan} = v_k^s (t_k^i - \tilde{t}_k^i) \tag{2.1}$$

shown on y-axis (the modulo of the LEB circumference) can be called the 'synchronizing phase'. For synchronous transfer, the synchronizing phase is equal to zero (ignoring the transfer line delays). We can readjust the trip_plan and arrange any point equal to the synchronous transfer point.

Since the MEB to LEB circumference ratio is 3960/570=6.9473684, which means when the frequencies are the same at the end of one MEB turn the LEB reference particle would have completed 6 full turns and a semi-turn. By adding this semi-turn 19 times, we get one full LEB turn. Hence, there will be 19 MEB turns before the LEB reference particle reaches the same reference point again.This is clearly visible in the trip-plan in Figure 3 above. The trip-plan calculated by Equation 2.1 is for an ideal synchronous particle. In the presence of field errors, the actual path covered by the reference particle is different and can be referred to as 'trip'. By ignoring the field errors in the MEB at the time of injection to the MEB (since the beam is assumed to be coasting at the top LEB frequency) for kth turn of the LEB, the trip is given by:

$$(\psi_k)_{Trip} = (v_k^s + \delta v_k)(t_k - \tilde{t}_k^i) \tag{2.2}$$

Here δv_k is the change in velocity from that of the synchronous particle and t_k is the actual traversal time of the LEB reference particle. The actual traversal time of the LEB reference particle is different from t_k^i used in Equation 2.1 above due to errors (Edwards and Syphers, 1990). It can be modelled by adding up the total traversal time required by the actual particle up to k turns as follows:

$$t_k = t_k^i - \sum_{n=1}^{k} \delta\tau_n \tag{2.3}$$

where $\delta\tau_k$ is the deviation with respect to the time taken by the synchronous particle in the LEB. The negative sign is due to the fact that, in the LEB (machine planned to operate below transition) a particle which has too much energy travels on a circle with greater radius, but is faster and hence takes shorter time to return to the gap than the ideal particle. By subtracting Equation 2.2 with Equation 2.1 the error in synchronizing phase can be obtained for kth turn as follows:

$$\delta\psi_k = -v_k^s\left(1 + \frac{\delta v_k}{v_k^s}\right)\sum_{n=1}^{k}\delta\tau_n + \left\{\frac{\delta v_k}{v_k^s}(\psi_k)_{Trip-plan}\right\} + \delta\psi_0 \tag{2.4}$$

To lock the LEB reference particle and the MEB reference bucket to the trip-plan we need to reduce the phase error, $\delta\psi_k$ to zero. $\delta\psi_0$ is the phase error we have deliberately created by selecting a given reference particle in the LEB. The deviation in the actual velocity of the particle for every MEB turn is generally small. That is the ratio $(\delta v_k)/v_k^s$ is small, if we chose enough samples in the trip-plan. Hence terms within the flower brackets can be ignored. Equation 2.4 is in difference equation form which can be converted to differential equation form by introducing τ^s as the traversal time of the ideal synchronous particle. While transforming to continuous domain the summation term is replaced by the integral. Hence the synchronization phase error is written as:

$$\delta\psi \cong -v^s \int \frac{\delta\tau}{\tau^s} dt \tag{2.5}$$

The synchronization model will be useful if we express in terms of the radial orbit shift and the dipole field error. This can be done by substituting the expression for the deviation in the traversal time in the presence of field errors (Bovet. C. et al, 1970). The resulting equation for the synchronization model is as follows:

$$\delta\psi = -v^s \int \left[\eta^s \gamma_T^2 \frac{\delta R}{R^s} - \frac{1}{(\gamma^s)^2} \frac{\delta B}{B^s} \right] dt + \delta\psi_0 \tag{2.6}$$

The superscript ' ^{s} ' is used to represent the parameters fo the ideal synchronous particle. Clearly, when the field error is zero, the synchronization phase error is due to the orbital deviation. The relationship between the phase error and orbital deviation is weighted by the slip factor, η^s. If we have synchronized the reference particle in the LEB to the trip-plan earlier in the cycle then smaller slip factor would be beneficial. It means the particle tries to stay on orbit.

2.2. Transverse Orbital Deviation

The mean orbital deviation is zero for an ideal synchronous particle. In the presence of field errors, it is not zero. A general model is required to describe the longitudinal dynamics associated with the orbital deviations. To obtain a differential equation with appropriate control in the presence of errors we need to use the energy equation shown in Reference (Edwards and Syphers). If $\overline{\Delta E}$ is the difference between the energy of the synchronous particle and the particle we are tracking, then,

$$\overline{\Delta E}_{k+1} = \overline{\Delta E}_k + (e(V_k^s + \delta V_k)\sin\phi_k - eV_k^s \sin(\phi_k)_0^s) \tag{2.7}$$

where δV_k is given by

$$\delta V_k = \delta V_k^c + \delta V_k^e \tag{2.8}$$

with δV_k^c as the control supplied to the cavity gap voltage and δV_k^e the error in the cavity voltage for kth turn and $(\phi_k)_0^s$ is the particle phase for the ideal synchronous case. ϕ_k is the particle phase of the non-synchronous case and V_k^s is the amplitude of the programmed voltage function for the synchronous particle. The quantity δV_k^c can be set to zero when we do not use global amplitude feedback. The energy equation is in finite difference form. It can be transformed to differential equation in the usual way, as follows.

$$\frac{d\delta E}{dt} = \frac{eV^s\beta^s c}{2\pi R^s} [(1 + \delta V^c + \delta V^e)\sin(\phi) - \sin(\phi_0^s)] \tag{2.9}$$

The particle phase, ϕ can be written in terms of the nominal synchronous phase, ϕ_0^s, the deviation from the synchronous phase representing the synchrotron oscillations, $\delta\phi^s$ and also, a phase shift, $\delta\phi^c$ as supplied by the controller. That is,

$$\phi = \phi_0^s + \delta\phi^c + \delta\phi^s \tag{2.10}$$

The phase shift $\delta\phi^c$ is used in the feedback strategy shown in Figure 1. It is well known in accelerators that

$$\delta E = (\beta^s)^2 \frac{\delta P}{P^s} E^s \tag{2.11}$$

The momentum change shown in Equation 2.11 can be expressed as:

$$\frac{\delta P}{P^s} = \gamma_T^2 \frac{\delta R}{R^s} - \frac{\delta B}{B^s} \tag{2.12}$$

Substituting Equation 2.12 in Equation 2.11 for the momentum change and by taking the first derivative of the resulting equation with respect to time, we get the following equation:

$$\frac{d\delta E}{dt} = \dot{A}_1 \delta R + A_1 \frac{d\delta R}{dt} + A_2 \frac{d\delta B}{dt} + \dot{A}_2 \delta B \tag{2.13}$$

where the coefficients, $\dot{A}_1$ and $\dot{A}_2$ are the first derivative of A_1 and A_2 and are shown in Table 1 below. Comparing Equations 2.13 and 2.9 and rewriting the resulting equation we get the desired equation for the radial orbital deviations as follows:

$$\frac{d\delta R}{dt} = \frac{A_3}{A_1} [(1 + \delta V^c + \delta V^e) \sin(\phi) - \sin(\phi_0^s)] - \frac{\dot{A}_1}{A_1} \delta R - \frac{A_2}{A_1} \delta \dot{B} - \frac{\dot{A}_2}{A_1} \delta B \tag{2.14}$$

where A_3 is the time varying coefficient of Equation 2.9 as shown in Table 1. Equation 2.14 combined with Equation 2.10 describes the dynamics of the orbital deviation.

2.3 The Particle Phase Model

For control purpose the longitudinal dynamics described by Equation 2.14 is incomplete without representing the synchrotron oscillations in terms of the controllable and measurable parameters. If f_k^s is the nominal frequency as programmed in the oscillator, δf_k^c is the control input generated by the controller and δf_k^e is the error in the oscillator itself, then the beam phase equation can be written as,

$$\phi_{k+1} = \phi_k + 2\pi (f_k^s + \delta f_k^c + \delta f_k^e)(\tau_k^s + \delta\tau_k) \tag{2.15}$$

Using equation for $\delta\tau_k$ in Equation 2.15 the following phase equation is obtained.

$$\frac{\phi_{k+1} - \phi_k}{\tau_k^s} = 2\pi (f_k^s + \delta f_k^c + \delta f_k^e) \left[1 + \eta_k^s \gamma_T^2 \frac{\delta R_k}{R^s} - \frac{1}{(\gamma_k^s)^2} \frac{\delta B_k}{B_k^s} \right] \tag{2.16}$$

Equation 2.16 can be written in the differential equation form by ignoring the second order terms as follows.

$$\frac{d\phi}{dt} = \frac{2\pi f^s \eta \gamma_T^2}{R^s}\delta R - \frac{2\pi f^s}{(\gamma^s)^2 B^s}\delta B + 2\pi f^s + 2\pi\delta f^c + 2\pi\delta f^e \tag{2.17}$$

The term $2\pi f^s$ can be ignored since it is multiples of 360 degrees. By substituting from equation 2.10 for the particle phase we get the following differential equation for the synchrotron oscillations,

$$\frac{d\delta\phi^s}{dt} = \frac{2\pi f^s \eta \gamma_T^2}{R^s}\delta R + 2\pi\delta f^c - \frac{d\delta\phi^c}{dt} - \frac{2\pi f^s}{(\gamma^s)^2 B^s}\delta B + 2\pi\delta f^e - \frac{d\phi_0^s}{dt} \tag{2.18}$$

It is useful to rewrite the control model in state space form and is done below.

2.4 State Space Model

The model shown in section 2.3 can be written in state space form by assuming the following definition for the measured quantities and the control inputs.

$$\begin{aligned} x_1 &= \delta\psi & u &= \delta f^c \\ x_2 &= \delta R & w &= \delta V^c \\ x_3 &= \delta\phi^s & & \\ x_4 &= \delta\phi^c & & \end{aligned} \tag{2.19}$$

In the above equation $\delta\psi$, δR, $\delta\phi^s$ are measured quantities (see Figure 1). Whereas, $\delta\phi^c$, is a control input used to shift the phase of the global RF signal. Also in our beam model the global frequency shift and the amplitude shift are represented by control inputs. The field shift, δB, cannot be considered like this, since we are not feeding any signal to the magnet system power supply from the global beam control system. Now, by using the new variables in Equation 2.6 we obtain the state space description for the synchronization model as follows:

$$\dot{x}_1 = a_{11}x_1 + a_{12}x_2 + d_{11}\delta B - a_{11}x_0 \tag{2.20}$$

where the time varying coefficients are tabulated in Table 1. Similarly, the state space description of the radial orbit shift can be obtained by substituting Equation 2.19 in Equation 2.14. After simplifying the algebra and rearranging the coefficients, we get the following non-linear equation.

$$\begin{aligned} \dot{x}_2 = {} & a_{22}x_2 + (a_{23} - \tilde{a}_{23}\omega)\sin(x_3 + x_4) + (a_{24} - \tilde{a}_{24}\omega)\cos(x_3 + x_4) \\ & + \tilde{a}_{24} + d_{21}\delta B + \tilde{d}_{21}\delta\dot{B} \end{aligned} \tag{2.21}$$

The time varying coefficients are shown in the Table 1. The state space description of the phase oscillations is given by substituting Equation 2.19 in Equation 2.18. Thus Equations 2.20 and 2.22 are linear and time varying. For synchrotrons such as the super col-

$$\dot{x}_3 = a_{32}x_2 + b_{31}u + v - \dot{\phi}_0^s + d_{31}\delta B + b_{31}\delta f^e$$
$$\dot{x}_4 = -v \tag{2.22}$$

lider, the time variation can be ignored. Whereas Equation 2.21 is non-linear in nature, but is linearizable for small operating region of x_3 and x_4. However, we show the design of the controllers for the non-linear beam model in the following section.

3.0 Sliding-Mode Controllers

The non-linear state space model described in Table 1 can be simplified to a third order system when we ignore the control going to the phase shifter i.e., $\delta\phi^c = 0$. Also, for the present controller design we ignore the global amplitude loop (i.e., $\omega = 0$). Hence the modified equation becomes equal to:

$$\dot{x}_1 = a_{11}x_1 + a_{12}x_2 + d_{11}\delta B - a_{11}x_0$$
$$\dot{x}_2 = a_{22}x_2 + a_{23}\sin(x_3) + a_{24}\cos(x_3) + \tilde{a}_{24} + d_{21}\delta B + \tilde{d}_{21}\delta\dot{B}$$
$$\dot{x}_3 = a_{32}x_2 + b_{31}u - \dot{\phi}_0^s + d_{31}\delta B + b_{31}\delta f^e \tag{3.1}$$

Our control objective is to stabilize the system and also drive the states, x_1, x_2 and x_3 on the average to zero in the presence of errors. Two sliding schemes can be applied to this problem with each having slightly different emphasis on the control objective.

3.1 Conventional Sliding-Mode Approach

In this scheme the sliding variable is defined as the linear combination of the states as follows:

$$\sigma = g_1x_1 + g_2x_2 + x_3 \tag{3.2}$$

Note that we normalized the coefficient of x_3 to 1. The reason is that the sliding plane is completely determined by g_1 and g_2 when $\sigma = 0$. Clearly, during sliding the variable σ=0. This means the states are confined to the sliding plane. If we chose right coefficients, g_1 and g_2, the states will be asymptotically converging to zero. Ideally, when the system is operating, we would need to have all the states driven to zero except for x_1 since we need x_1 to be zero only at the time of transfer. However, due to the way σ is chosen eventhough there is synchronism (i.e. $x_1 = 0$), x_2 and x_3 may not be zero in the presence of field error (see Equations 3.1). The design of the controller proceeds as follows.

Differentiate Equation 3.2 and substitute Equation 3.1 in the resulting equation, we get:

$$\dot{\sigma} = g_1a_{11}x_1 + (g_1a_{12} + g_2a_{22} + a_{32})x_2 + g_2(a_{23}\sin x_3 + a_{24}\cos x_3 + \tilde{a}_{24}) + b_{31}u +$$
$$(g_1d_{11} + g_2d_{21} + d_{31})\delta B + g_2\tilde{d}_{21}\delta\dot{B} - g_1a_{11}x_0 - \dot{\phi}_0^s + b_{31}\delta f^e \tag{3.3}$$

Now select the control input, u as follows

$$u = u_c + u_s \tag{3.4}$$

where,:

$$u_c = -\frac{1}{b_{31}}[g_1 a_{11} x_1 + (g_1 a_{12} + g_2 a_{22} + a_{32}) x_2 + g_2 (a_{23}^0 (\sin x_3 + a_{24}^0) \cos x_3 + \tilde{a}_{24})]$$

$$u_s = -\frac{1}{b_{31}}[k_0 + k_3 |x_3|] \operatorname{sgn}\sigma$$

Since a_{23} and a_{24} contains δV^e term we had to chose the nominal values a_{23}^0 and a_{24}^0 respectively in the continuous part of the control input. In the switching part of the control input x_3 is assumed to be less than 1 radians (true for the LEB). The gains, k_0 and k_3 help to overcome the errors. They are chosen as follows.

$$k_0 > sup\left|g_1 d_{11}\delta B - a_{11}x_0 + (d_{21} + d_{31})\delta B + \tilde{d}_{21}\delta\dot{B} - \dot{\phi}_0^s + b_{31}\delta f^e + g_2\frac{A_3}{A_1}\delta V^e \sin\phi_0^s\right|$$

$$k_3 > sup\left|g_2\frac{A_3}{A_1}\delta V^e \cos\phi_0^s\right| \qquad (3.5)$$

Hence the sliding condition:

$$\sigma\dot{\sigma} < 0 \qquad (3.6)$$

Even if Equation 3.6 is satisfied for all time the system may not be stable, but is confined to the sliding plane. This is because our control problem is multistate. If we choose the coefficients of the sliding plane, g_1 and g_2 properly then the system asymptotically converges to origin. When the system is sliding x_3 can be expressed in terms of other two states, which is obtained by substituting $\sigma = 0$ in Equation 3.2. Thus:

$$x_3 = -g_1 x_1 - g_2 x_2 \qquad (3.7)$$

By substituting Equation 3.7 in the Equation for x_3 in Equation 3.1 we get the following second order system.

$$\begin{aligned} \dot{x}_1 &= a_{11}x_1 + a_{12}x_2 + d_{11}\delta B - a_{11}x_0 \qquad (3.8) \\ \dot{x}_2 &= a_{22}x_2 + a_{23}\sin(-g_1x_1 - g_2x_2) + a_{24}\cos(-g_1x_1 - g_2x_2) + \tilde{a}_{24} + d_{21}\delta B + \tilde{d}_{21}\delta\dot{B} \end{aligned}$$

To analyze the stability of this reduced-order non-linear system, we can use the theorem from the reference (Slotine and Li, 1990). According to the theorem, if we linearize Equation 3.8 and show that the linear system is asymptotically stable, then the non-linear counterpart is locally stable. Hence to analyze the stability linearized equations of 3.8 are given below:

$$\begin{aligned} \dot{x}_1 &= a_{11}x_1 + a_{12}x_2 + d_{11}\delta B - a_{11}x_0 \\ \dot{x}_2 &= -a_{23}g_1x_1 + (a_{22} - a_{23}g_2)x_2 + d_{21}\delta B + \tilde{d}_{21}\delta\dot{B} \end{aligned} \qquad (3.9)$$

For stability of the linear system all the roots of the characteristic equation must lie in the left half of the s-plane for all time i.e.,

$$\textit{Real Parts of roots of det } (s\underline{I} - \underline{A}) < 0$$

and the following definite integral is bounded due to the time varying coefficients.

$$\int_{0}^{0.05} \underline{A}^{T}(t)\,\underline{A}(t)\,dt < \infty \tag{3.10}$$

Applying Equation 3.10 we come up with the following conditions on g_1 and g_2:

$$g_1 < -\frac{(a_{11} + a_{22})}{a_{23}} \quad , \qquad g_2 > \frac{(g_2 a_{11} a_{23} - a_{11} a_{22})}{a_{12} a_{23}} \tag{3.11}$$

The coefficients g_1 and g_2 must satisfy Equation 3.11 and are chosen to get appropriate time constant in the loop, because during sliding they represent the time constant of the closed loop system.

3.2 Generalized Input-State Linearization and Sliding-Mode Control

The input-state linearization technique (Hunt, Su, Meyer, 1983) is well known for the control community. The technique is useful to design the controllers for non-linear systems without the uncertainties. They deal with only the non-linear autonomous systems and is not robust. Hence we have come up with a possible generalized design which can handle the non-autonomous case and also in the presence of uncertainties the system is robust. The robustness is achieved by using sliding-mode techniques.

Definition 1:
An n-th order non-autonomous system in the form,

$$\begin{aligned} \dot{\underline{x}} &= f(\underline{x}, t) + g(\underline{x}, t)\,u \\ y &= h(\underline{x}) \end{aligned} \tag{3.12}$$

is said to be of relative degree r in the region Ω if, for all $\underline{x}$ in Ω, we require r times differentiation on y in order for control u to appear. The relative degree is set to be well defined if the coefficient of u in the rth derivative of y is non-zero in the region Ω.

Definition 2:
An n-th order system in the form of,

$$\dot{\underline{x}} = f(\underline{x}, t) + g(\underline{x}, t)\,u \tag{3.13}$$

is said to be input-state linearizable in the generalized sense if there exists a region Ω in R^n, a diffeomorphism T: $\Omega \rightarrow R^n$, and a non-linear time-varying feedback control law

$$u = \alpha(\underline{x}, t) + \beta(\underline{x}, t)\,\upsilon \tag{3.14}$$

such that the new state variable $\underline{z} = T(\underline{x})$ and the new control input υ satisfy a linear time invariant relation

$$\dot{\underset{\sim}{z}} = \underset{\sim}{A}\underset{\sim}{z} + \underset{\sim}{b}\upsilon \tag{3.15}$$

where

$$\underset{\sim}{z} = \begin{bmatrix} z_1 \\ z_2 \\ z_3 \\ \vdots \\ z_n \end{bmatrix}_{n \times 1} \qquad \underset{\sim}{A} = \begin{bmatrix} 0 & 1 & 0 & \cdots & 0 \\ 0 & 0 & 1 & \cdots & 0 \\ 0 & 0 & 0 & \cdots & 0 \\ \vdots & \vdots & \vdots & \cdots & \vdots \\ 0 & 0 & 0 & \cdots & 0 \end{bmatrix}_{n \times n} \qquad \underset{\sim}{b} = \begin{bmatrix} 0 \\ 0 \\ 0 \\ \vdots \\ 1 \end{bmatrix}_{n \times 1}$$

The new input υ is the linear control to stabilize Equation 3.15. The final system shown by Equation 3.15 is in the form known as Brunovsky Form (Brunovsky, 1970) which is simply the extra state transformation of the non-linear non-autonomous state Equation 3.13.

In definition 1 we have chosen y as the output. Whereas in our system we do not have one specific output. Hence we define any state as the output, say, $y = z_1(\underset{\sim}{x}) = z_1(x_1)$. By following definition 1, we see that the system Equation 3.13 is input-state linearizable when the relative degree of $z_1(x_1)$ is known and if the coefficient of u appearing in rth derivative of $z_1(x_1)$ is non-zero. The relative degree is found out by applying the transformation shown in definition 2.

$$\begin{aligned} \dot{z}_1 &= \dot{x}_1 = a_{11}x_1 + a_{12}x_2 = z_2 \\ \dot{z}_2 &= \ddot{x}_1 = (a_{11}^2 - \dot{a}_{11})x_1 + (a_{11}a_{12} + a_{12}a_{22} + \dot{a}_{12})x_2 + a_{23}\sin(x_3) + a_{24}\cos(x_3) \\ &= z_3 \\ \dot{z}_3 &= \dddot{x}_1 = F(\underset{\sim}{x}, t) + G(\underset{\sim}{x}, t)\,u \end{aligned} \tag{3.16}$$

where $F(\underset{\sim}{x}, t)$ is a complicated function of the states and $G(\underset{\sim}{x}, t)$ is given by:

$$\begin{aligned} G(\underset{\sim}{x}, t) &= 2\pi g_2 \frac{A_3}{A_1} a_{12}\cos(\phi_0^s + x_3)\left(1 + \frac{\delta V^e}{V}\right) \\ &= G^0\left(1 + \frac{\delta V^e}{V}\right) \end{aligned} \tag{3.17}$$

In developing Equation 3.16, the system Equations 3.1 is used to replace the derivatives of the system states. Clearly, in the third derivative of z_1, u appears. Hence, the relative degree of the system is three. Also, since z_1 being the output has the degree equal to the order of the system (see Equation 3.1), the state equations are input-state linearizable. According to definition 2 to cancel out the non-linearities in z_3 we can chose u as follows:

$$u = -\frac{F(\underset{\sim}{x}, t)}{G(\underset{\sim}{x}, t)} + \frac{1}{G(\underset{\sim}{x}, t)}\upsilon \tag{3.18}$$

The resulting system is in the Brunovsky form. z_1, z_2 and z_3 become the new states of the transformed linear system.

Remark:
From definition 2, we see that an nth order system in the form of Equation 3.13 is input-state linearizable if there exists a function $z(\underset{\sim}{x})$ such that the relative degree of system with $z(\underset{\sim}{x})$ as output has a relative degree of n.

All three equations in 3.16 are in the companion form (Slotine 1984). If we know the parameters exactly then we can use the non-linear control, u as in Equation 3.18 to cancel all the non-linearities. However, in practice we have the system uncertainties and disturbances. By applying the sliding-mode controller to the system equation in companion form we can achieve robustness in the loop. To design the controller we can define the sliding line in the usual form in terms of the output, z_1 as follows:

$$\begin{aligned} \sigma &= z_3 + c_1 z_2 + c_2 z_1 \\ &= \ddot{z}_1 + c_1 \dot{z}_1 + c_2 z_1 \end{aligned} \tag{3.19}$$

It is natural to define the sliding line as the linear combination of the new linearized states z_1, z_2 and z_3. With this we would be driving the synchronization phase error zero. Since during sliding, $\sigma = 0, z_1 = x_1 = 0$. By virtue of the fact that $x_1 = 0$, the other states will be zero.

Now by differentiating the sliding variable and using Equation 3.16 we get the following equation.

$$\begin{aligned} \dot{\sigma} = {} & \gamma_1 x_1 + \gamma_2 x_2 + \gamma_3 \sin x_3 + \gamma_4 \cos x_3 + G a_{32} x_2 + \\ & \zeta_1 \delta B + \zeta_2 \delta \dot{B} + \beta_2 \delta \ddot{B} + d_{31} G (\delta B - \dot{\phi}_s^0 + b_{31} u) \end{aligned} \tag{3.20}$$

where γ_1, γ_2, γ_3 and γ_4 are given by:

$$\begin{aligned} \gamma_1 &= \dot{\alpha}_1 + \alpha_1 a_{11} + c_1 \alpha_1 + c_2 a_{11} \\ \gamma_2 &= \dot{\alpha}_2 + \alpha_1 a_{12} + c_1 \alpha_2 + c_2 a_{12} + \alpha_2 a_{22} \\ \gamma_3 &= \dot{\alpha}_3 + \alpha_2 a_{23} + c_1 \alpha_3 \\ \gamma_4 &= \dot{\alpha}_4 + \alpha_2 a_{24} + c_1 \alpha_4 \end{aligned} \tag{3.21}$$

The variables ζ_1, ζ_2, α_1, α_2, α_3 and α_4 are shown below in terms of the machine parameters:

$$\begin{aligned} \zeta_1 &= \dot{\beta}_1 + \alpha_1 d_{11} + \alpha_2 d_{21} + c_1 \beta_1 + c_2 d_{11} \\ \zeta_2 &= \dot{\beta}_2 + \alpha_2 \tilde{d}_{21} + c_1 \beta_2 + \beta_1 \\ \alpha_1 &= a_{11}^2 + \dot{a}_{11} \\ \alpha_2 &= a_{11} a_{12} + \dot{a}_{12} + a_{12} a_{22} \\ \alpha_3 &= a_{12} a_{23} \\ \alpha_4 &= a_{12} a_{24} \end{aligned} \tag{3.22}$$

with β_1 and β_2 given by:

$$\begin{aligned} \beta_1 &= a_{11} d_{11} + \dot{d}_{11} + a_{12} d_{21} \\ \beta_2 &= d_{11} + a_{12} \tilde{d}_{21} \end{aligned} \tag{3.23}$$

To guarantee stability we need to define u such that:

$$u = \frac{-1}{G^o b_{31}} [u_c + u_s \operatorname{sgn}(\sigma)] \tag{3.24}$$

with u_c and u_s as continuous and switching parts defined as below:

$$u_c = \gamma_1 x_1 + (\gamma_2 + G^o a_{32}) x_2 + \gamma^o{}_3 \sin(x_3) + \gamma_4^o(\cos(x_3) - 1)$$

$$u_s = H + sup\left(\left|\frac{\delta V^e}{V^s}\right|\right)(H + |u_c|) \tag{3.25}$$

where

$$H > \left|(\gamma_3 - \gamma_3^0)\sin(x_3) + (\gamma_4 - \gamma_4^0)(\cos(x_3) - 1) + (G - G^0) a_{32} x_2\right| \tag{3.26}$$

Under sliding $\sigma = 0$. Substituting this condition in Equation 3.19 we can get the time domain solution for z_1, which in turn gives x_1, an exponentially decaying state with a final value equal to zero. Thus, under sliding, x_1, $\dot{x}_1$, $\ddot{x}_1$ tend to zero. A simple analysis of the original system equation 3.1 will show that x_2, $\dot{x}_2$ and x_3 will tend to zero on the average in the presence of noise.

4. Implementation

Equations 3.4 and 3.24 are sliding-mode controllers with time-varying gains. For hardware implementation, it amounts to storing all the gains in the computer and fetching them during each processing point on real time. This increases the computational time. In any case the analog implementation will be difficult with time varying gains though not impossible. Hence it is useful to simplify the controllers. One way of doing this is to plot all the gains with respect to time and take the mean values. The deviation from the mean value is being taken care of by the gains in the switching part which contributes to the robustification of the loop in the presence of errors. For the LEB parameters shown in the reference (Mestha, Kwan, Yeung, 1991), we calculated the controllers with fixed gains. They are summarized in Table 2 below. In this table we show two types of state feedback controllers. They are shown to compare the results of the sliding-mode controllers. Loop configurations are shown in Figures 4 and 5. In addition to the state feedback loops, the system needs robustifying loops with gains shown in Table 2. The implementation of this type of simplified robust controllers does not look far from reality due to the advancement in Direct Digital Synthesizers and Digital Signal Processor technology. Especially for machines like the MEB and the HEB we can afford the computational time spent on the robustifying loops.

5. Simulation Studies

Simulations were carried out with controllers shown in Table 2 for different conditions. At first we discuss the possible source of errors below.

5.1 Description of Expected Errors

Source of errors in the beam control loops are many and depend on the type of implementation. However, for the configuration shown in Figure 1, we have identified the errors expected during implementation. They are shown below.

Field Error:
Magnetic field errors could be due to the noise in the power supply driving the magnet system, or the vibration in the magnets. It is usually, multiples of power line frequency. Gaussian noise of bandwidth 1 kHz with a natural distribution is used. The amplitude of the random noise is considered 0.1% for the field signal. The cavity-voltage error, δV^e, cannot be ignored in the LEB. A 1% error in the magnitude with a 50 kHz bandwidth (uncorrelated with the magnetic field error) Gaussian noise is a good representation to the practical system.

$$\begin{aligned} dB &= 10 \times 10^{-4} \times B^s(t) \times rand(normal) \\ \delta V^e &= 1 \times 10^{-2} \times V^s(t) \times rand(normal) \end{aligned} \tag{4.1}$$

Measurement Error in Radial Position:
A radial beam position measurement system planned for the LEB would be able to give a minimum horizontal position of 0.1 mm from the central orbit. By using a 12 bit Analog to Digital Converter we extracted the radial position information from the tracking model. The sampling was done at each MEB turn and the samples were taken with each least significant bit corresponding to 0.1 mm.

Systematic and Random Errors in Beam Phase Measurements:
The random errors in the beam phase measurement were taken 1 % with a bandwidth of 20KHz which is close to the LEB synchronous frequency. The noise is again uncorrelated with other noise functions mentioned above. The systematic error is expected to arise when the measured beam phase is compared with the synchronous phase, ϕ_0^s, since the synchronous phase may not be calculated accurately. We assumed a systematic error of 2 ^{o}.

Errors in the Frequency Source:
Stability of the oscillator is very important for operating the LEB. An oscillator such as the Voltage Controlled Oscillator would have an analog signal at the input which is subjected to noise. Fluctuations in frequency of as much as 200 Hz is not uncommon. A 20KHz bandwidth noise was used with maximum of ±200 Hz frequency error, δf^e.

Errors in the TDC:
The Time to Digital Converters are not ideal. We assumed a measurement error of $3ns$ amounting to 0.9cms phase error in the synchronization. A 10KHz bandwidth noise was used in the simulation.

Errors while ramping the Frequency:
After injecting the beam in the LEB, the frequency must be ramped between 47MHz-60MHz with a profile required by the synchronous particle. Starting point of the ramping is obtained by detecting the minimum magnetic field. However, there could be error in detecting the minimum field by as much as $100\mu s$. This will create a wrong starting point for the frequency ramp, and hence the programmed frequency curve is no longer equivalent

to the frequency ramp required by the magnetic field. We used $100 \mu s$ ramping error in the simulation.

5.2 Summary of Simulated Results

To illustrate the results, we show in Figures 6(a-d) the decay of the states x_1 x_2 x_3 and x_4 for control inputs with state-feedback controllers of Figure 1. In Figure 6(e) the control input u is shown. The particle we tracked was 30 meters away from the reference point at $t = 0$. We chose the sampling interval of 1 MEB turn (which is equal to $13.249 \mu s$). The tracking model we chose was in finite-difference form as shown in Reference (Mestha, Kwan, Yeung, 1991). Since the bunch contains several particles we need to know whether the particle with a maximum initial phase offset could get tracked into the same bucket. Hence we have shown in Figure 6(f) the difference in phase of the offset particle with the synchronous phase. This information is useful to know whether there is any particle loss. These figures are shown with and without errors. The initial offset with respect to the RF signal was $\pm 170°$, but receiving the same control input as in Figure 6(e). Particles over $\pm 170°$ did not remain in the same bucket. Figures 7 (a-e) are shown to represent the states, control input and the phase difference for the modified state feedback controller. The control input shown in Table 2 is obtained for a third order system. It is clear from the simulation results that the state feedback controller does not give synchronism in the presence of errors. We investigated the main cause for this. It turns out that the loops are sensitive to systematic phase error in the beam phase loop (state x_3). When we add the robustifying loops we see a different performance in the synchronization.

Figure 8(a-f) correspond to the states, control input and the sliding variable for the conventional state feedback controller shown in Table 2. Clearly we see that the synchronism is in order in the presence of errors. We could track the particle upto $\pm 169°$. Those particles above this either fell into the next bucket or got lost. Figures 9(a-f) correspond to the simulation results for controller designed with input-state linearization technique. Clearly, the robustification for systematic error is good for the synchronous particle. However, the particle with a phase offset of not more than $\pm 50°$ was contained in the same bucket.

6. Conclusions

The new method of phase-locking the Low Energy Booster with the Medium Energy Booster is analysed by deriving a beam control model in the presence of errors. The model is multistate and non-autonomous. It gives a good indication of the difficulties in designing controllers to guarantee stability. We have shown the design of two types of sliding-mode controllers. In the course of attempting to synchronize a given reference bunch in the LEB with a stable bucket in the MEB, the controllers not only damp the coherent dipole oscillations, but can also keep the radial beam orbit under control. The simulation results are compared with two types of state feedback controllers. The synchronization results with the state feedback controllers are shown to be not good in the presence of systematic errors. However, the results look very good when we apply the sliding-mode techniques. All the simulations were carried out using a single particle tracking code with the finite difference model as the beam and applying different feedback strategies at each MEB turn. We also tracked a particle with a large phase offset compared to the synchronous particle and applied the control generated for the synchronous particle to see whether it gets tracked inside the bucket in the presence of errors. With the state feedback controllers we see that a particle with an offset in phase by $\pm 170°$ gets tracked into the bucket. With the conventional sliding-mode we could track upto $\pm 169°$. The modified sliding-mode based on input-state linearization technique allows tracking of particles upto $\pm 50°$. The reason for failure in the modified sliding-mode case is due to the enhancement in noise in the numerical differentiation of the synchronization phase error. In all our simulations we assumed that the RF cavities have fast loop response compared to the global loops. Work is still required to assess the effects of Q of the resonant cavities. To implement the sliding-mode controllers with the modern day technology we either need to use fast Digital Signal Processors combined with Direct Digital Synthesizers or convert all the loops to analogue domain.

7. Acknowledgements

We thank Bob Webber and Richard Talman for their contributions to the technical discussions about the new synchronization scheme.

References

Bovet, C., *etal,* 1970, A Selection of Formulae and Data Useful for the Design of A.G. Synchrotrons, CERN Report CERN/MPS-SI/Int. DL/70/4.

Brunovsky, P., 1970, A Classification of Linear Controllable Systems, Kybernetika, 6, pp 173-188.

Edwards, D.A., and Syphers, M.J., 1990, An Introduction to the Physics of Particle Accelerators, SSC Laboratory Publication, Dallas, Texas.

Hunt. L.R., Su. R., and Meyer. G., 1983, IEEE Trans Automatic Control, 28, 24.

Mestha, L.K., 1991, Beam Control Feedback Loops for the Low Energy Booster, SSCL Report, SSCL-559, Superconducting Super Collider Laboratory, Dallas, Texas; 1991, Phase-Locked Loop with Controlled Phase Slippage, U.S. Patent Application, DOE Case No.: S-74,282.

Mestha, L.K., Kwan, C.M., and Yeung, K.S., 1991, Instabilities in Beam Control Feedback Loops in Proton Synchrotrons, Journal of Particle Accelerators, (To be published).

Slotine, J.J.E., and Li, W., 1990, Applied Nonlinear Control, Prentice Hall, New Jersey.

LIST OF TABLES

LIST OF FIGURES

Table 1: State Space Model

Non-Linear State Space Model:

$$\dot{x}_1 = a_{11}x_1 + a_{12}x_2 + d_{11}\delta B - a_{11}x_0$$

$$\dot{x}_2 = a_{22}x_2 + (a_{23} - \tilde{a}_{23}\omega)\sin(x_3 + x_4) + (a_{24} - \tilde{a}_{24}\omega)\cos(x_3 + x_4) + \tilde{a}_{24} + d_{21}\delta B + \tilde{d}_{21}\delta\dot{B}$$

$$\dot{x}_3 = a_{32}x_2 + b_{31}u + v - \dot{\phi}_0^s + d_{31}\delta B + b_{31}\delta f^e$$

$$\dot{x}_4 = -v$$

Time Varying Coefficients:

$$a_{11} = \frac{\dot{v}^s}{v^s} \qquad \tilde{a}_{23} = -\frac{A_3}{A_1}\cos\phi_0^s \qquad d_{11} = \frac{v^s}{(\gamma^s)^2 B^s}$$

$$a_{12} = -\frac{v^s \eta^s \gamma_T^2}{R^s} \qquad a_{24} = \frac{A_3}{A_1}(1 + \delta V^e)\sin\phi_0^s \qquad d_{21} = -\frac{\dot{A}_2}{A_1}$$

$$a_{22} = -\frac{\dot{A}_1}{A_1} \qquad \tilde{a}_{24} = -\frac{A_3}{A_1}\sin\phi_0^s \qquad \tilde{d}_{21} = -\frac{A_2}{A_1}$$

$$a_{23} = \frac{A_3}{A_1}(1 + \delta V^e)\cos\phi_0^s \qquad a_{32} = \frac{2\pi f^s \eta^s \gamma_T^2}{R^s} \qquad d_{31} = \frac{2\pi f^s}{(\gamma^s)^2 B^s}$$

$$b_{31} = 2\pi$$

$$A_1 = \frac{(\beta^s)^2 \gamma_T^2 E^s}{R^s} \qquad A_2 = \frac{(\beta^s)^2 E^s}{B^s} \qquad A_3 = \frac{eV^s \beta^s c}{2\pi R^s}$$

Variables:

$x_1 = \delta\psi \qquad x_2 = \delta R \qquad x_3 = \delta\phi^s \qquad u = \delta f^c \qquad \omega = \delta V^c$

Errors: $\delta B \quad \delta f^e \quad \delta V^e$

Table 2: Summary of the Feedback Controllers

State-Feedback Controller as in Figure 1:

$$u = -(30x_1 + 1000x_2)$$

$$x_4 = -\int (1000x_2 - 20x_4)\, dt$$

Modified State-Feedback Controller:

$$u = -(25x_1 + 1000x_2 + 5000x_3)$$

Conventional Sliding-Mode Controller:

$$\sigma = g_1 x_1 + g_2 x_2 + x_3$$

$$u = -(25x_1 + 10^7 x_2 + 10^4 x_3 + u_s)/2\pi$$

$$u_s = (30|x_1| + 10^6|x_2| + 10^4|x_3| + 250)\ \mathrm{sgn}\sigma$$

$$g_1 = 2.5, \quad g_2 = 5000$$

$\delta = 0.5$ - For saturation function

Modified Sliding-Mode Controller:

$$\sigma = \ddot{x}_1 + c_1 \dot{x}_1 + c_2 x_1$$

$$u = -(0.015x_1 + 2 \times 10^6 x_2 + 10^3 x_3 + u_s)$$

$$u_s = (0.002|x_1| + 10^6|x_2| + 500|x_3| + 150)\ \mathrm{sgn}\sigma$$

$$c_1 = 3200, \quad c_2 = 5 \times 10^5$$

$\delta = 5 \times 10^5$ - For saturation function

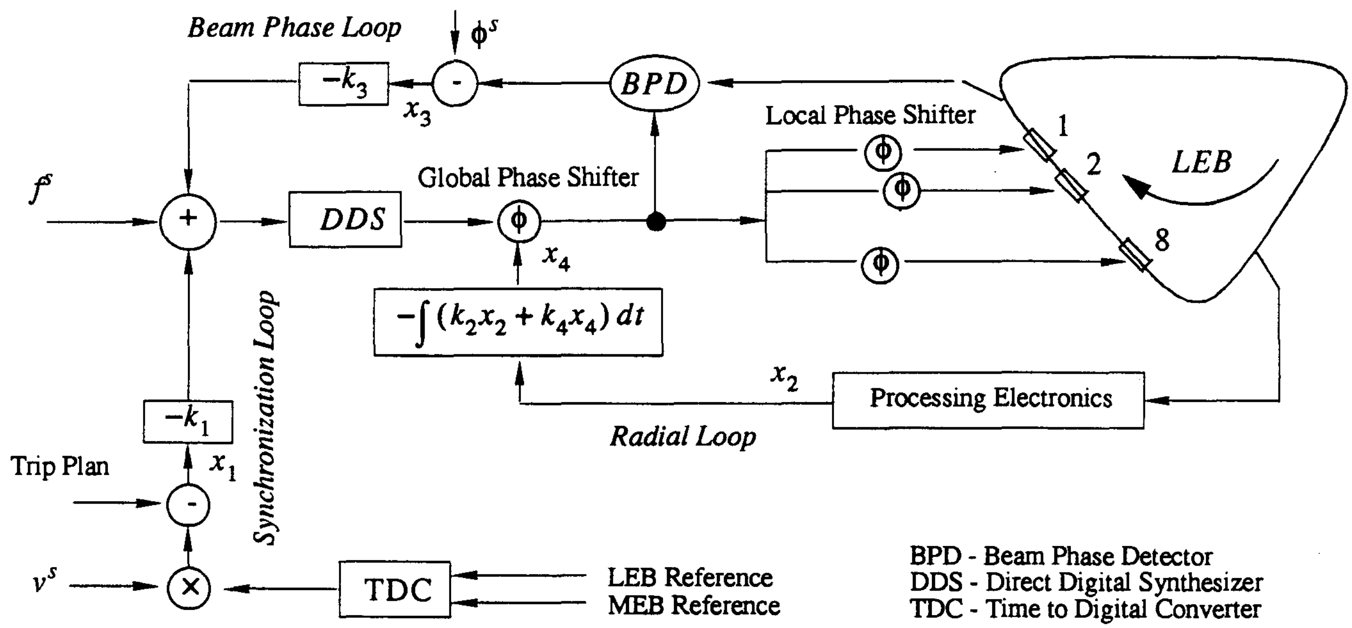

Figure 1. Schematic Representation of the Global Beam Control Feedback Loops for the LEB

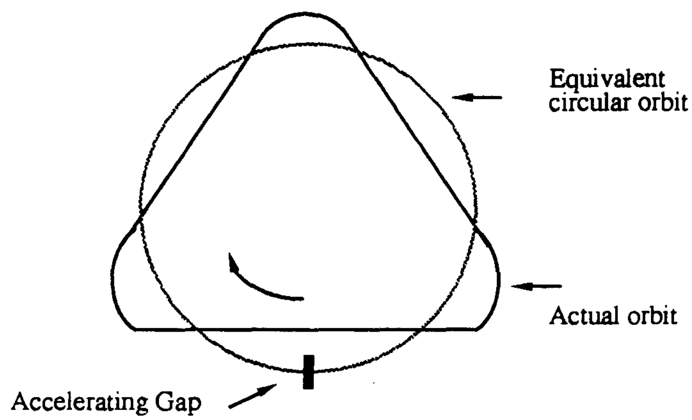

Figure 2. Schematic Representation of the actual orbit and the equivalent orbit.

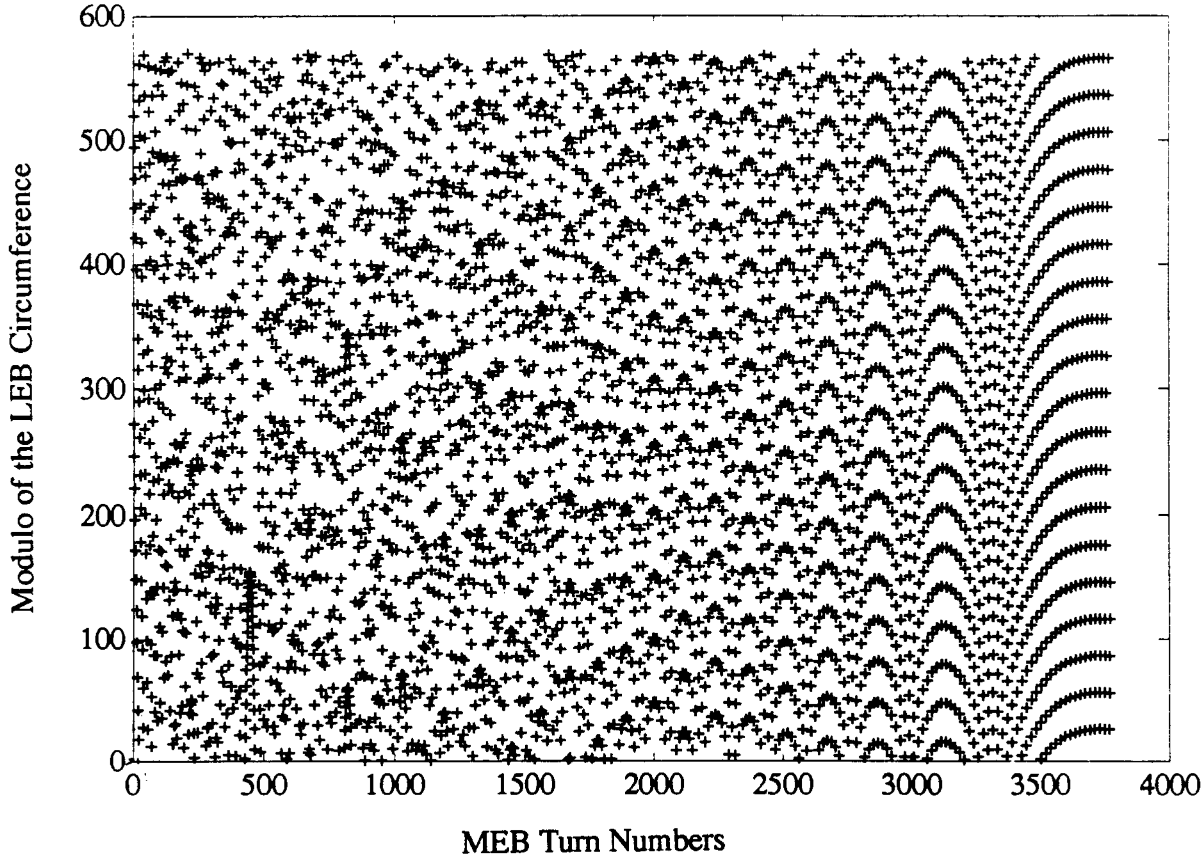

Figure 3. LEB Trip_Plan

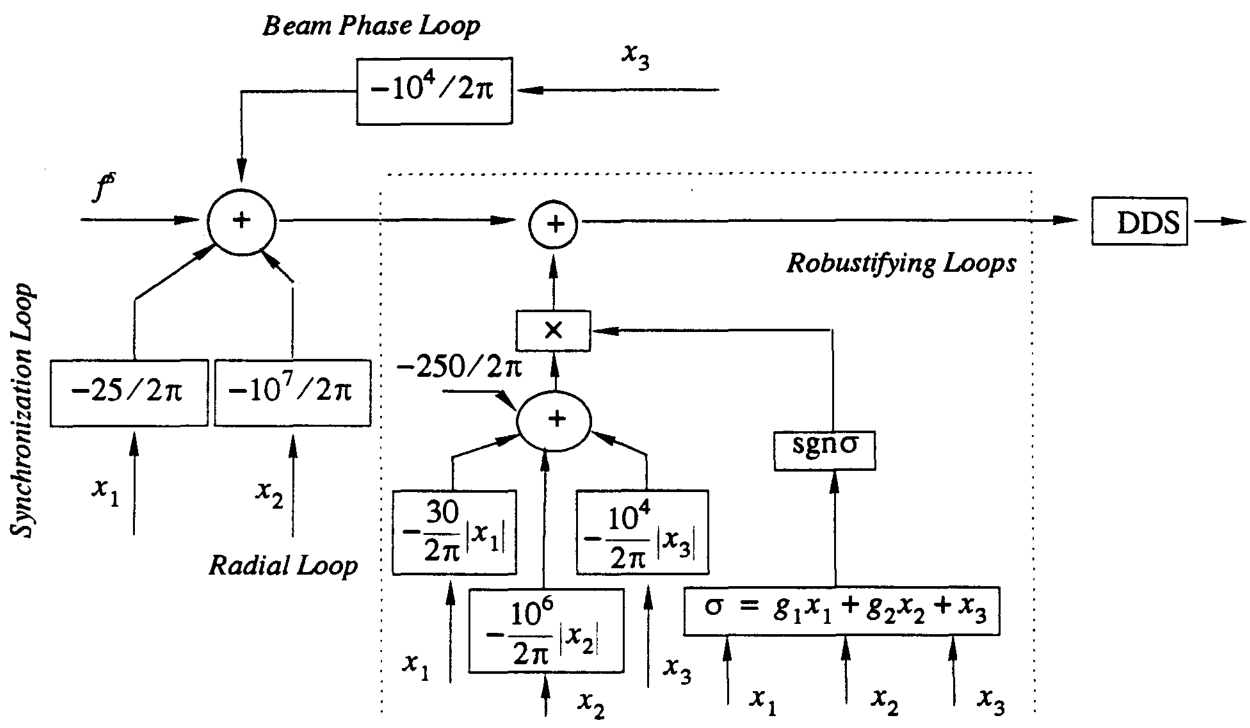

Figure 4. Schematic Representation of the Conventional Sliding-Mode Controller

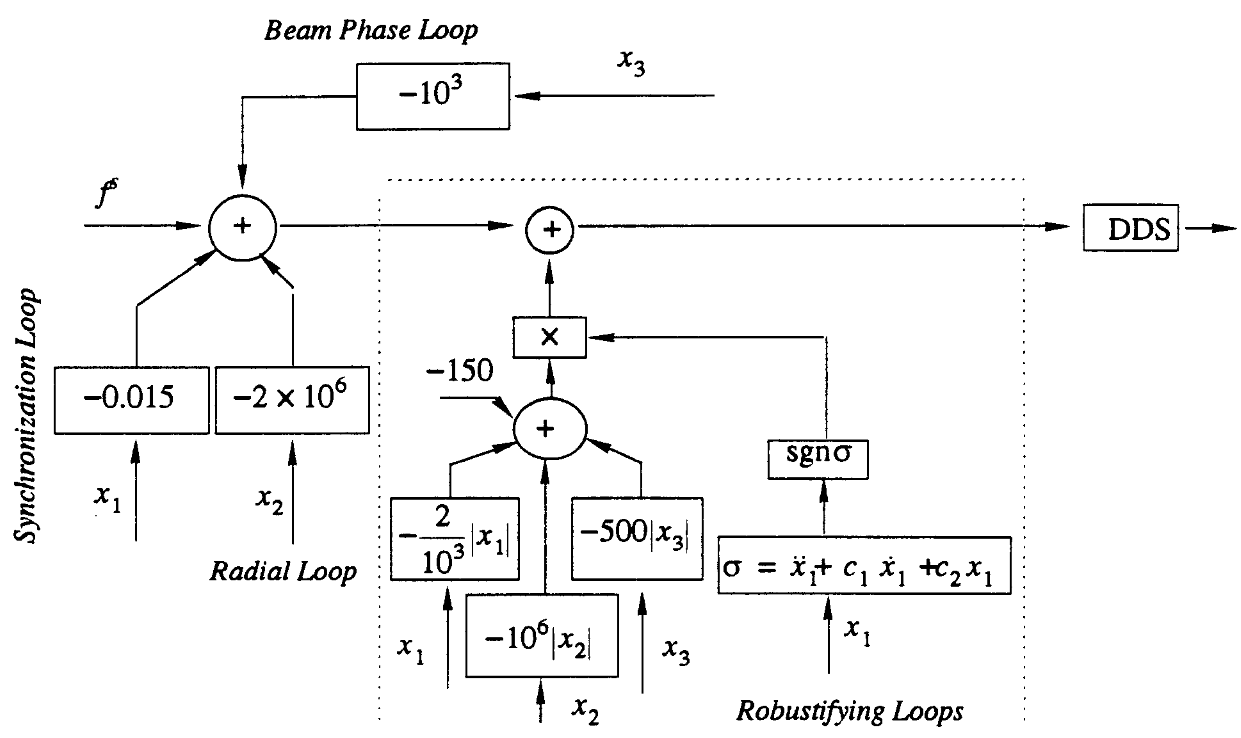

Figure 5. Schematic Representation of the Modified Sliding-Mode Controller

Figure 6(a)

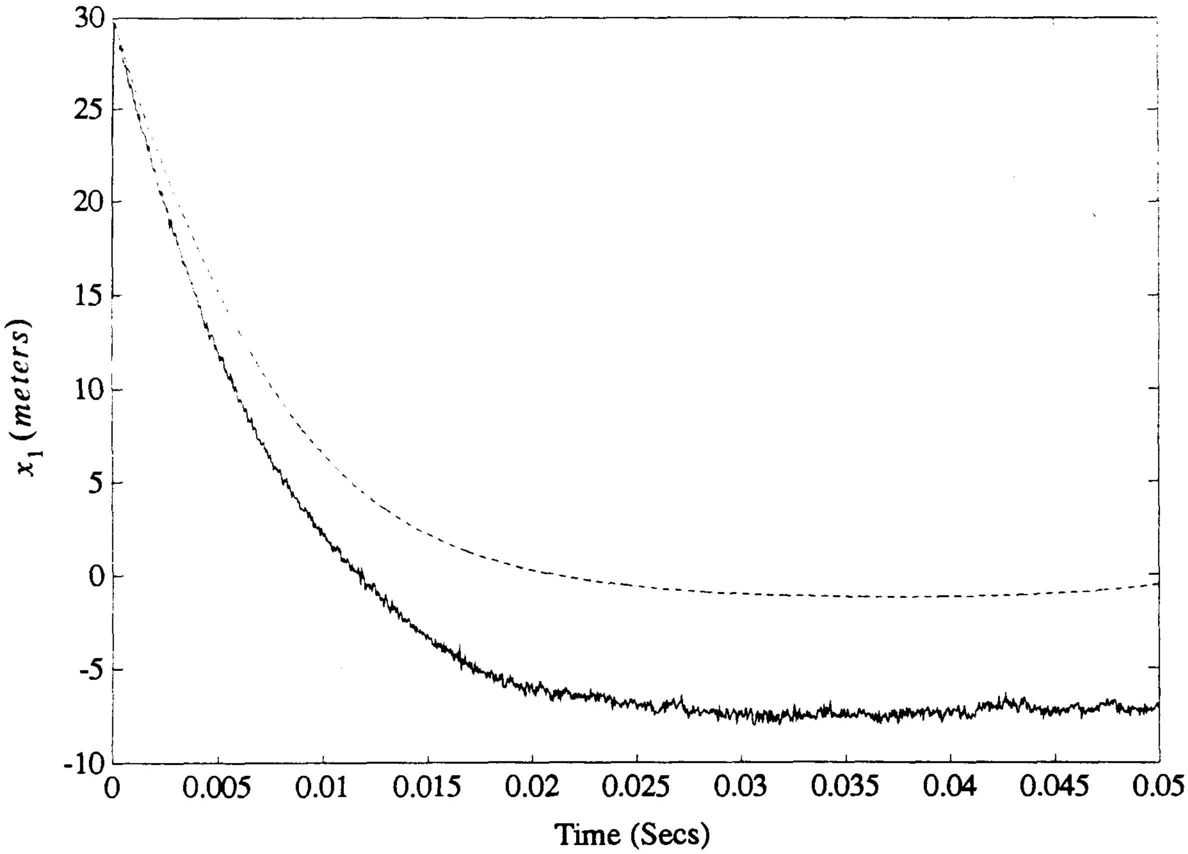

- - - - - Without Errors
——— With Errors

Figure 6(b)

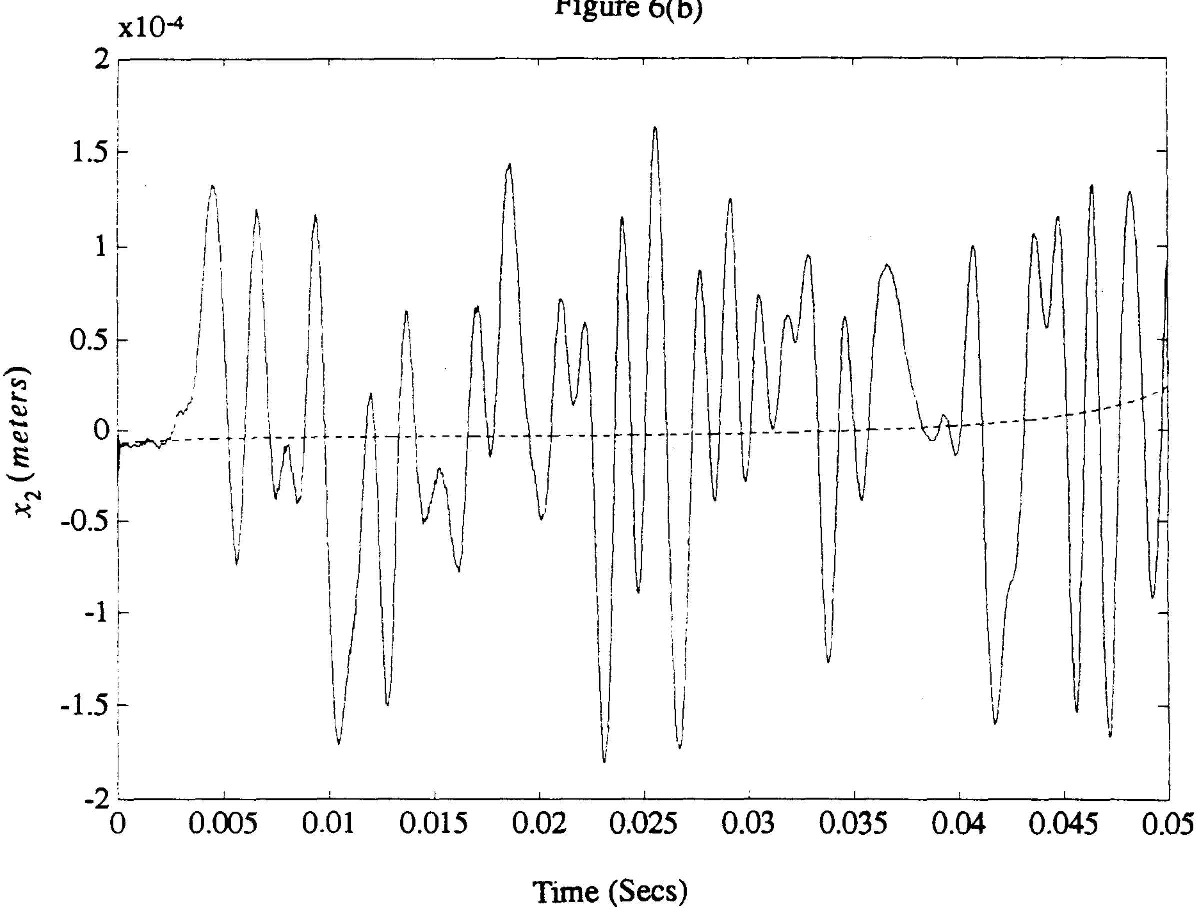

Figure 6(c)

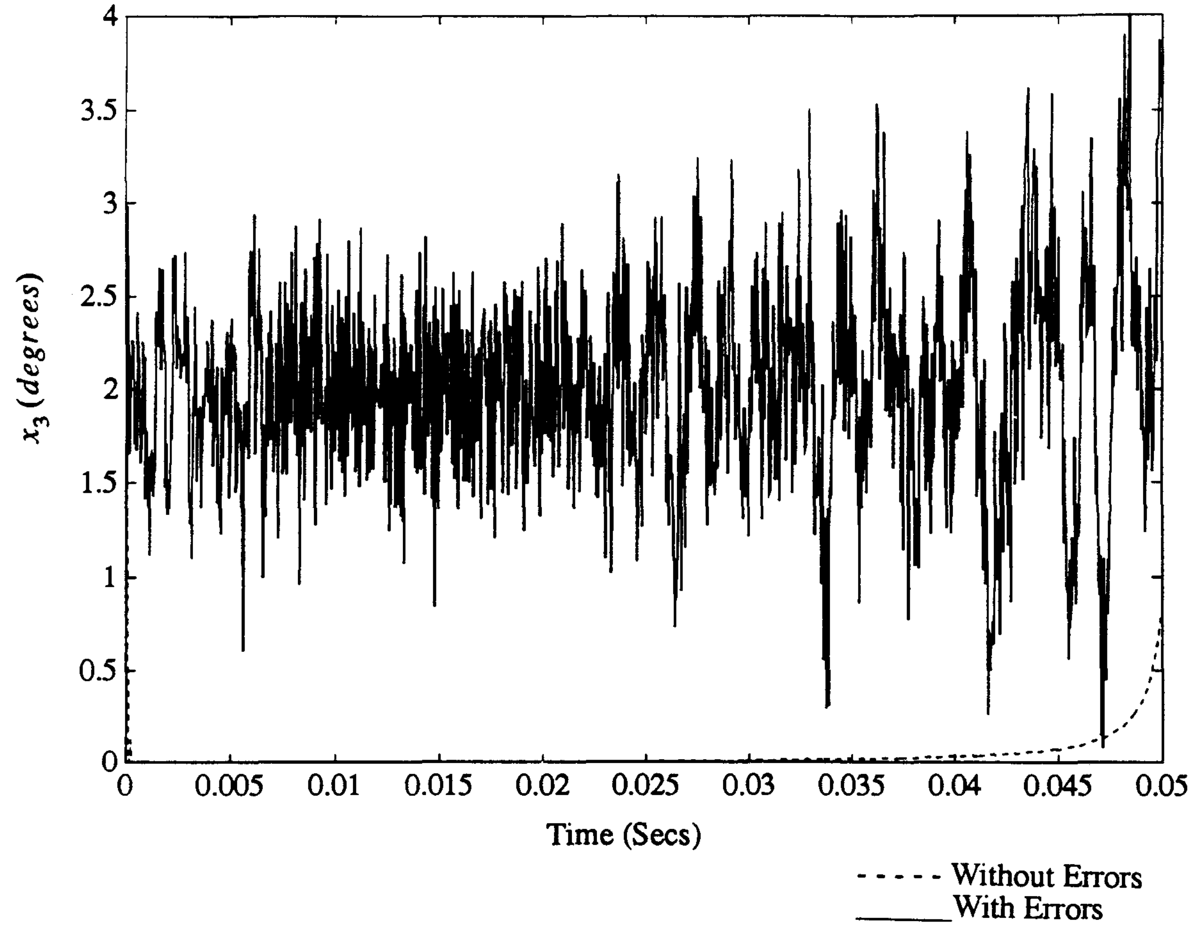

Figure 6(d)

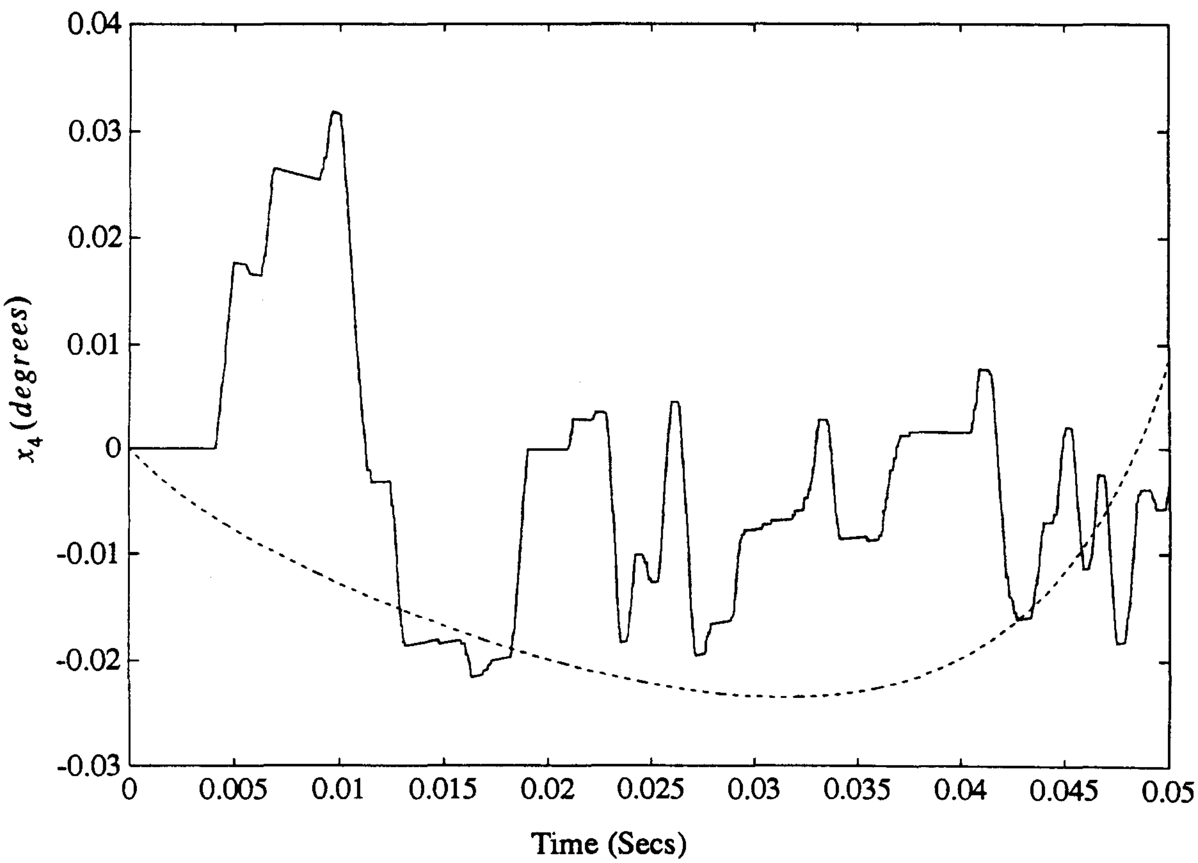

Figure 6(e)

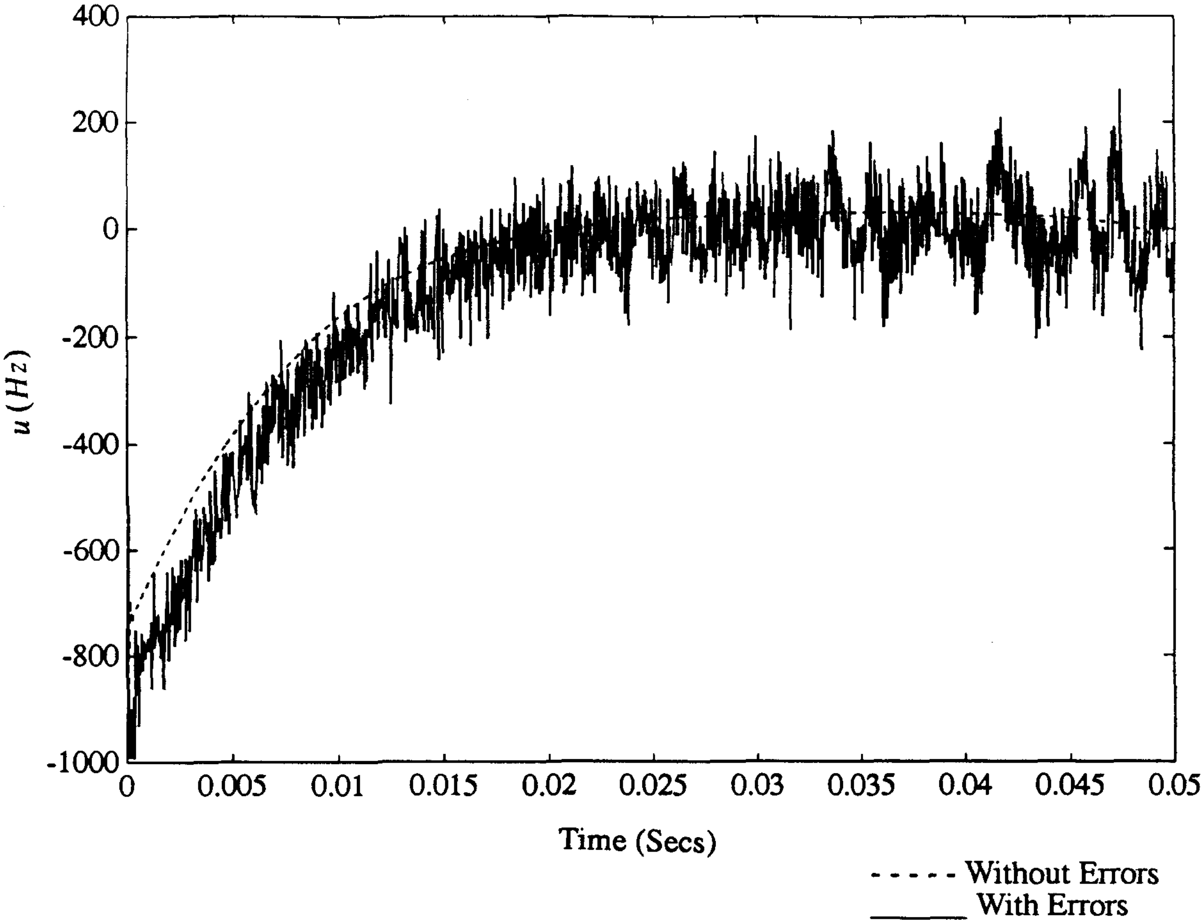

Figure 6(f)

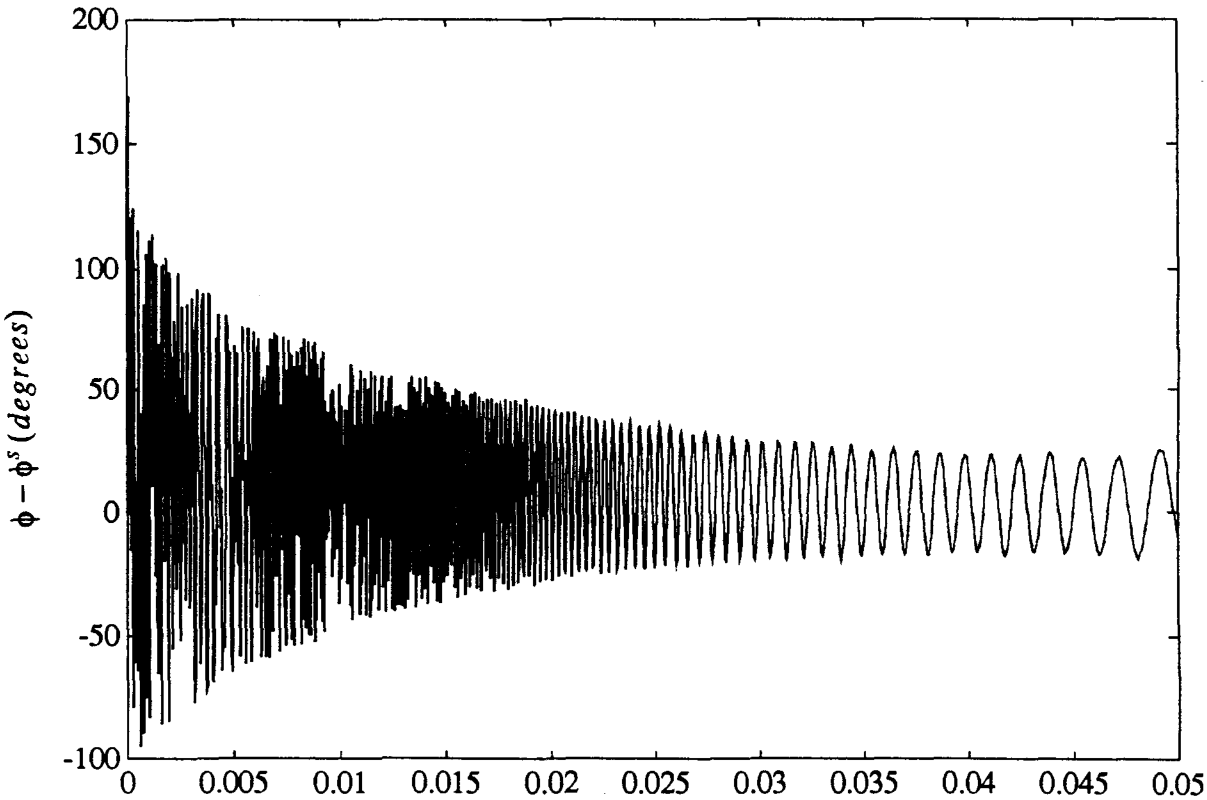

Figure 6. Simulation results for the state feedback controller of Figure 1
(a) Synchronization phase error (b) Radial orbit shift (c) Beam phase error
(d) Global phase shift (Control input) (e) Frequency shift (Control input)
(f) Phase difference of the offset particle

Figure 7(a)

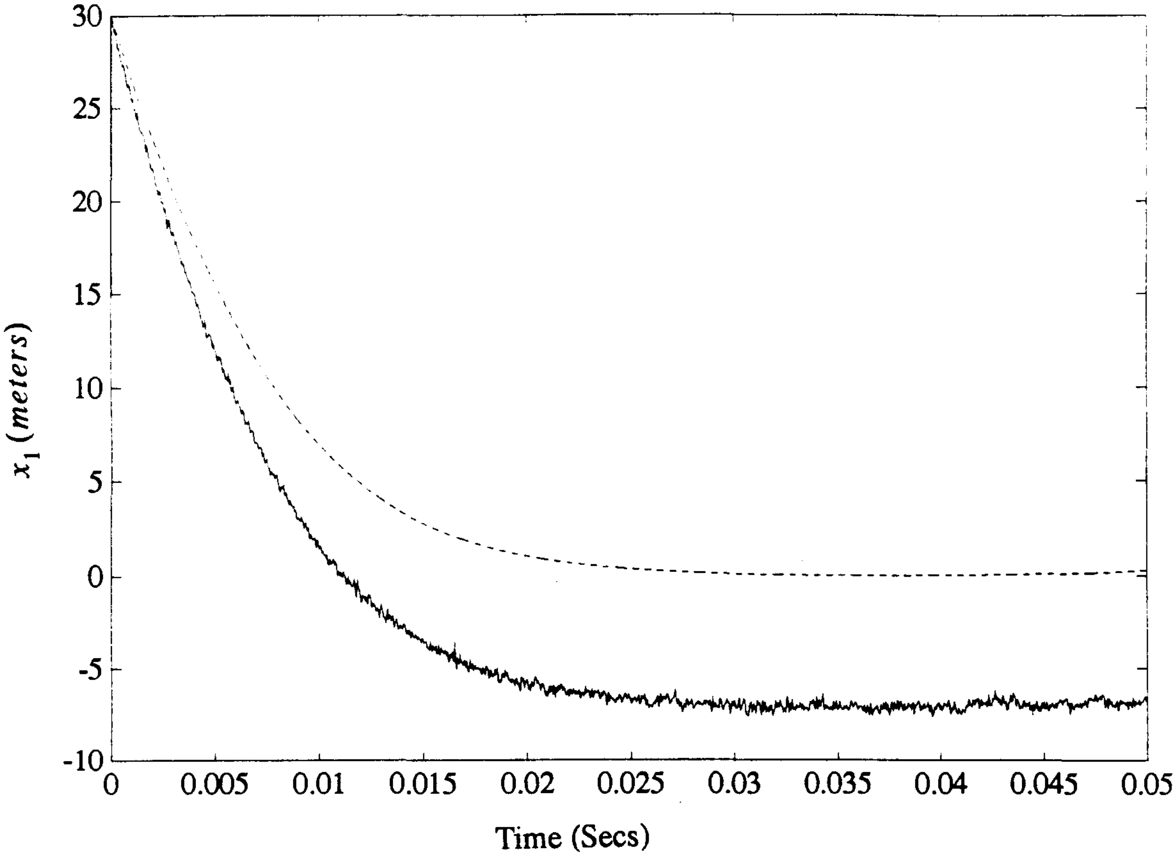

- - - - - Without Errors
_______ With Errors

Figure 7(b)

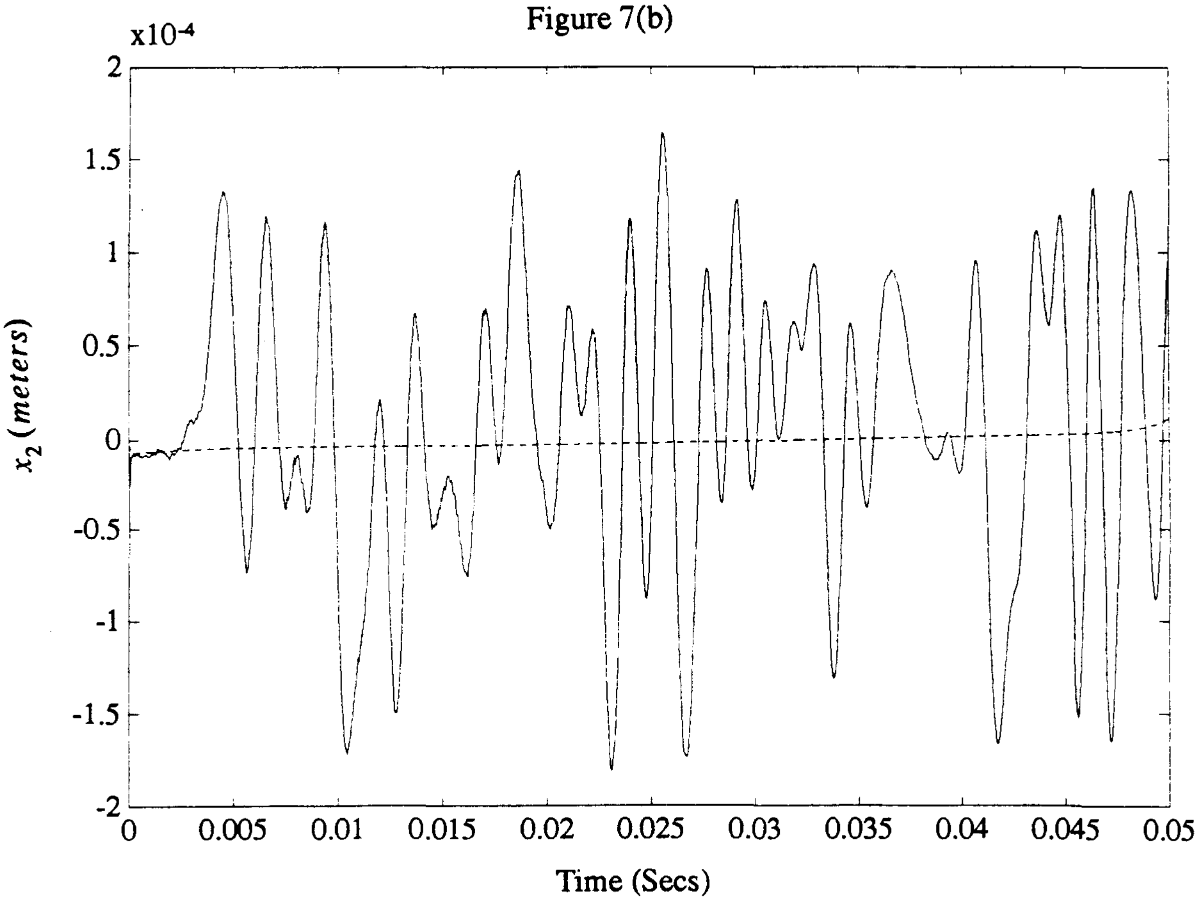

Figure 7(c)

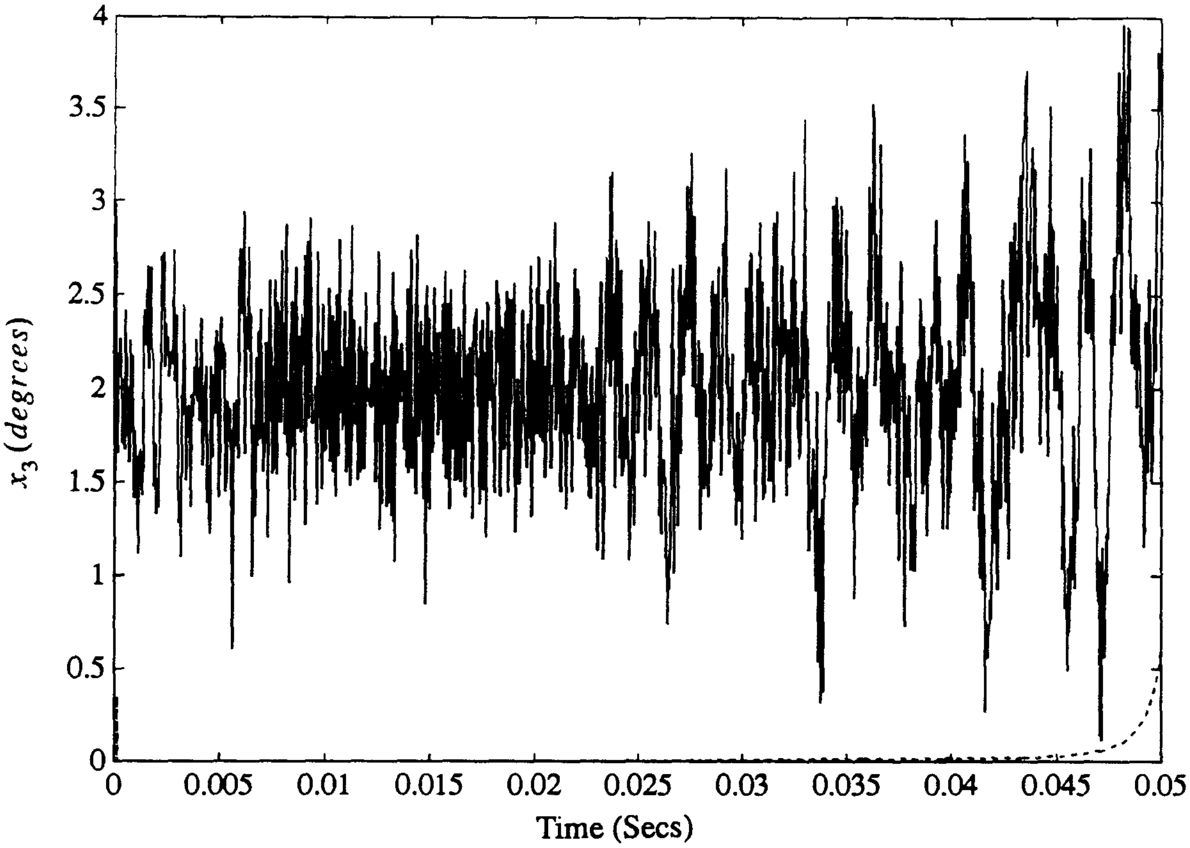

- - - - - Without Errors
______ With Errors

Figure 7(d)

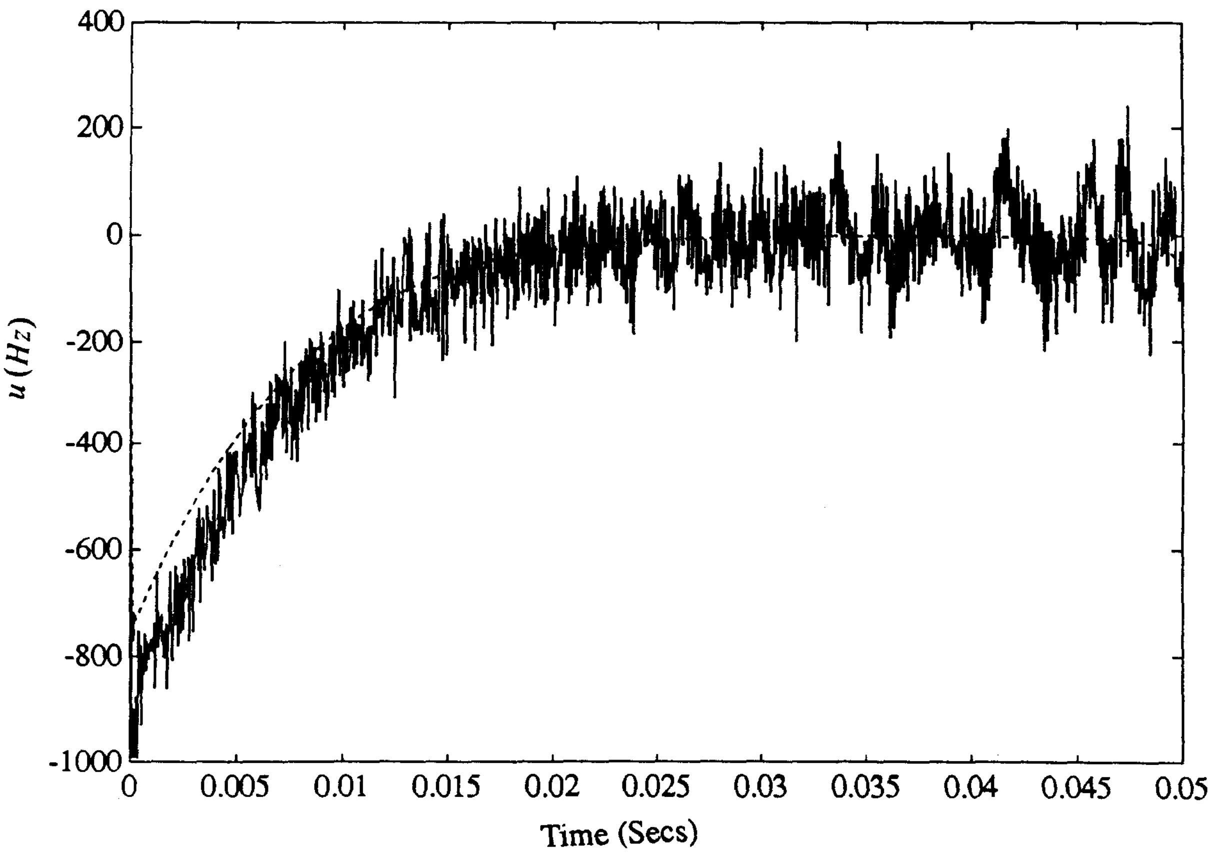

Figure 7(e)

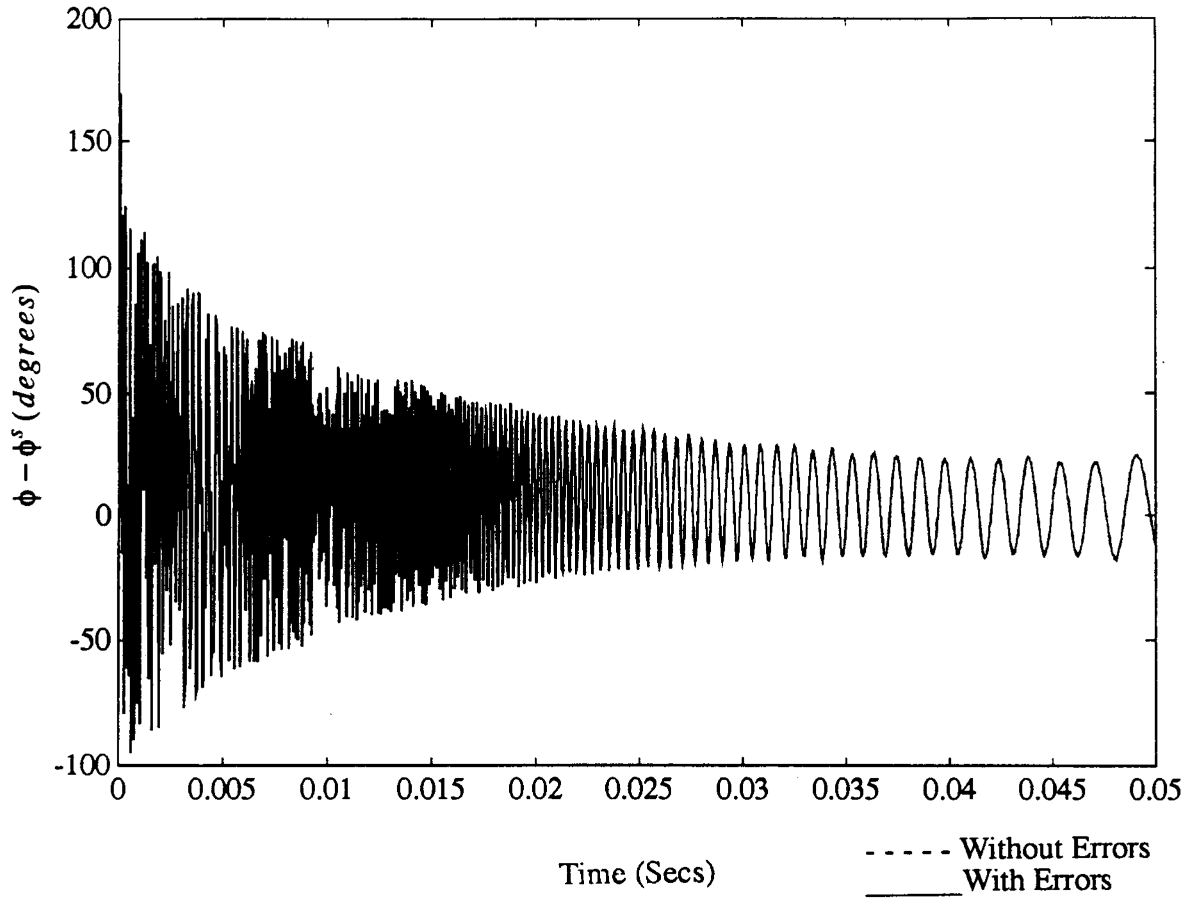

Figure 7. Simulation results for the modified state feedback controller
(a) Synchronization phase error (b) Radial orbit shift (c) Beam phase error
(d) Frequency shift (Control input) (e) Phase difference of the offset particle

Figure 8(a)

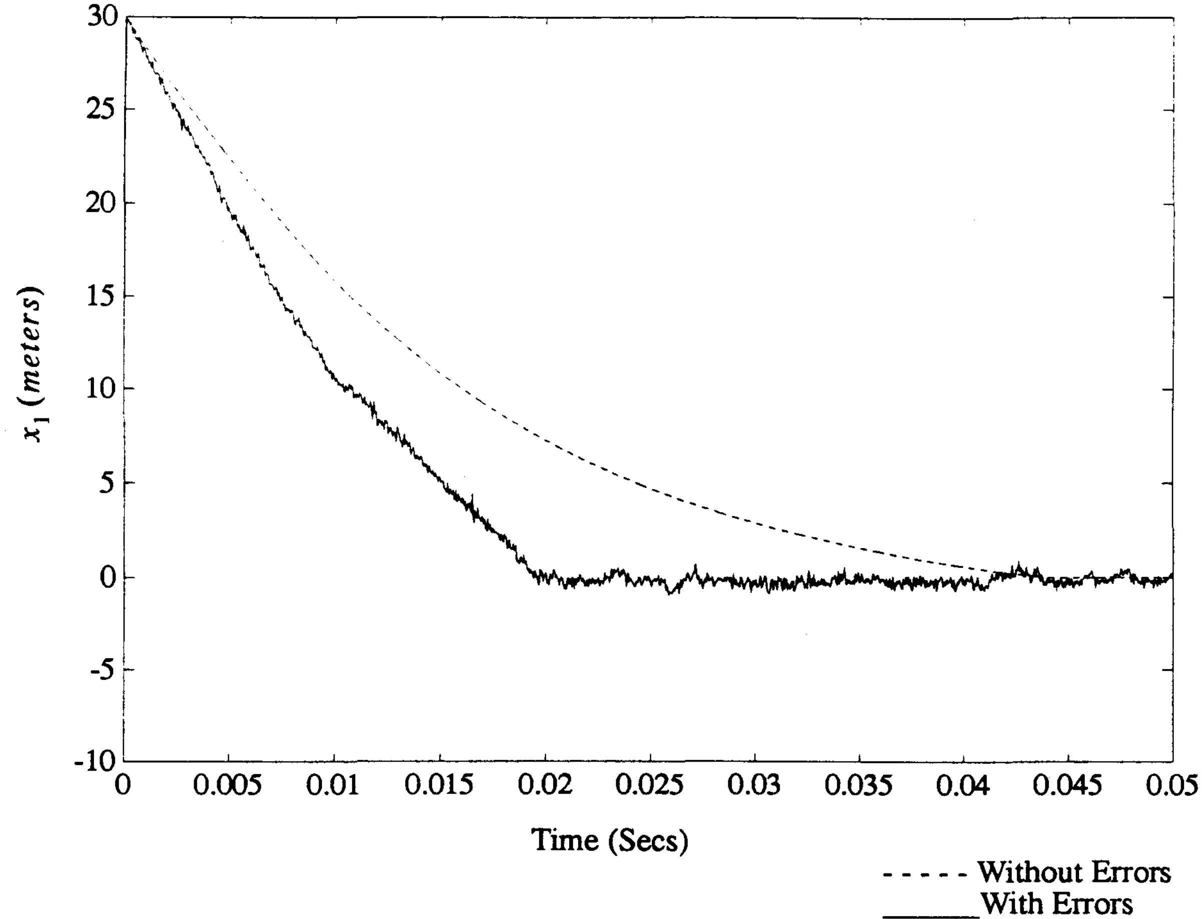

Figure 8(b)

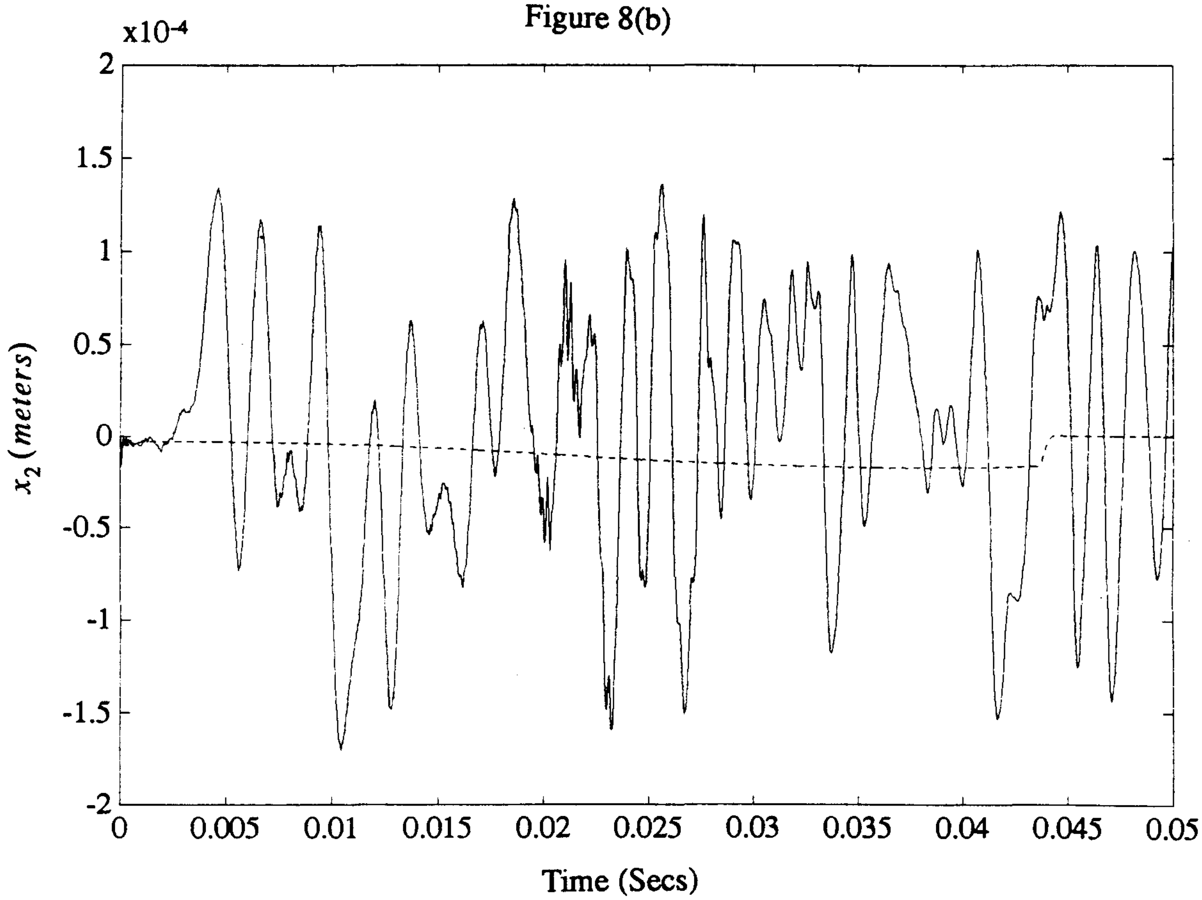

Figure 8(c)

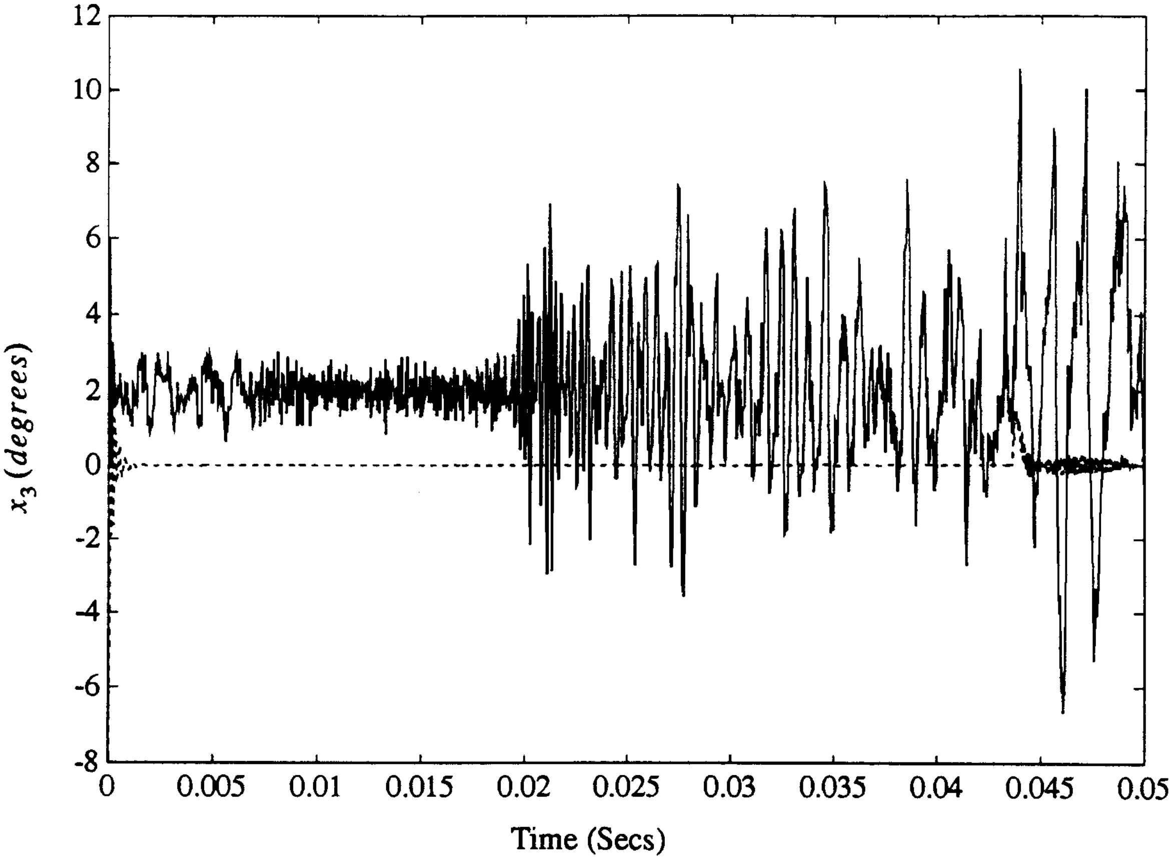

- - - - - Without Errors
______ With Errors

Figure 8(d)

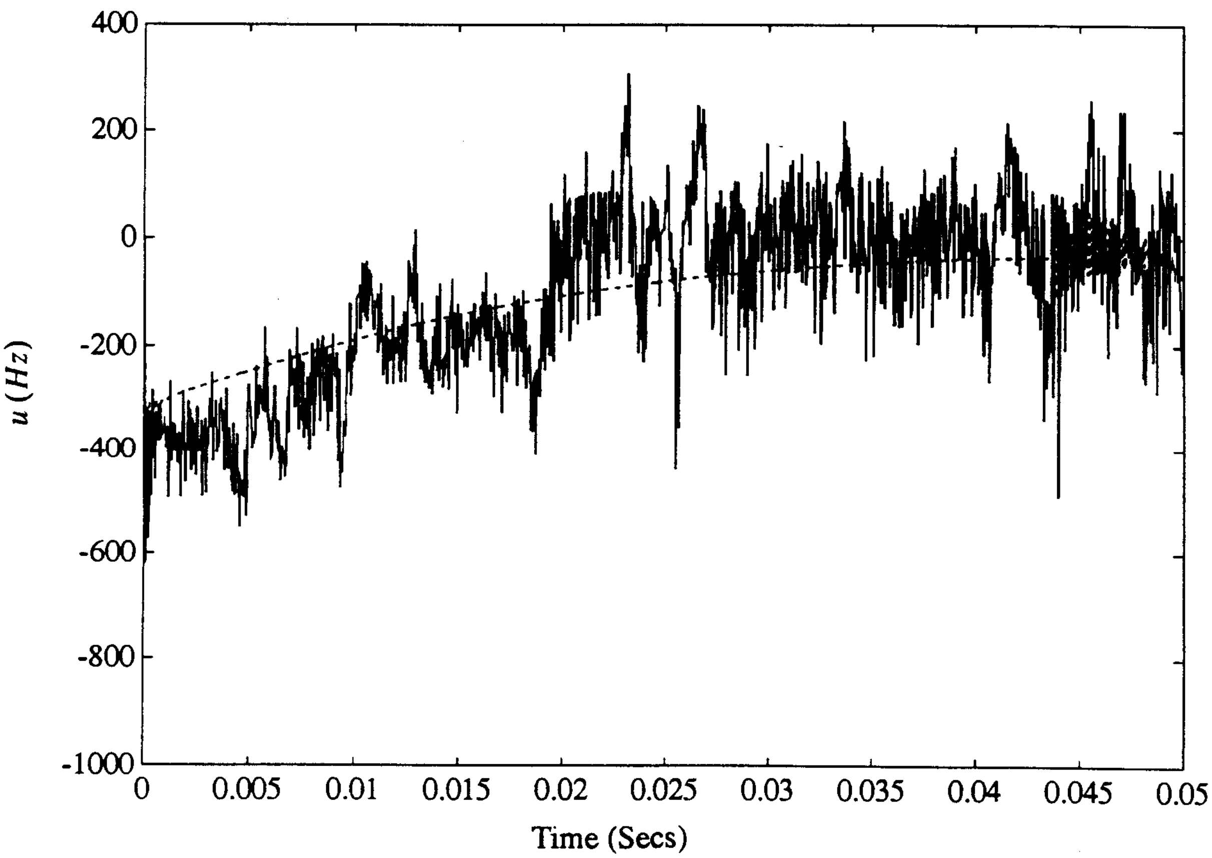

Figure 8(e)

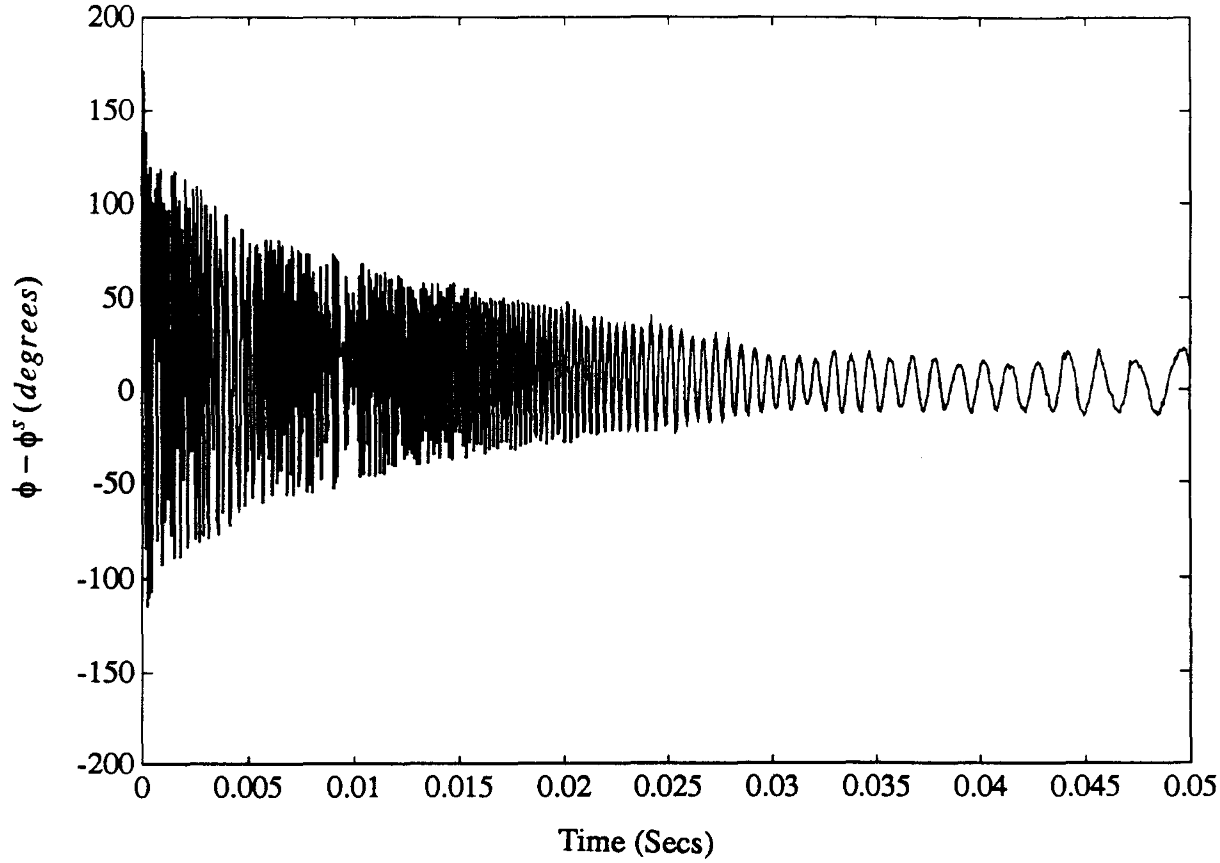

Figure 8(f)

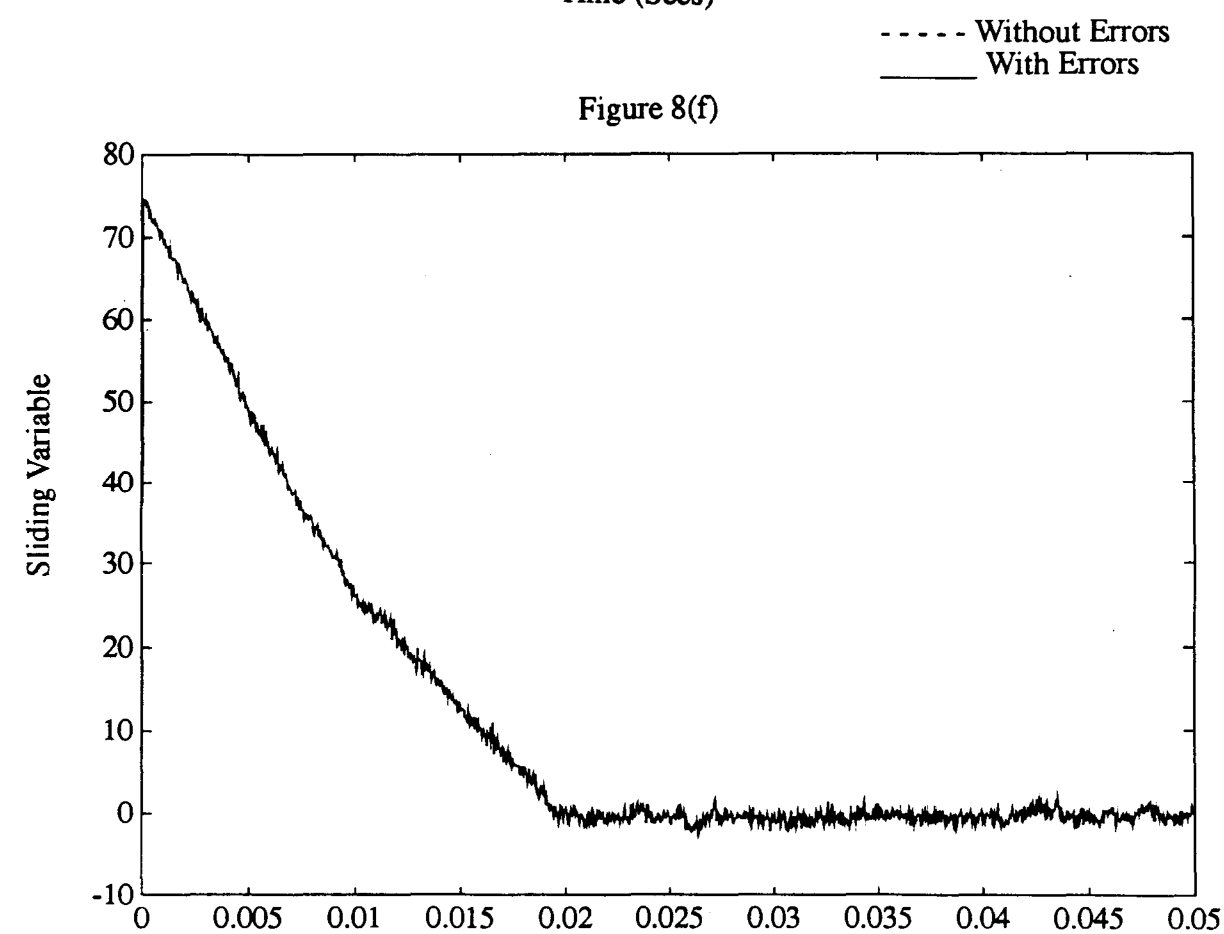

Figure 8. Simulation results for the conventional sliding-mode controller (a) Synchronization phase error (b) Radial orbit shift (c) Beam phase error (d) Frequency shift (Control input) (e) Phase difference of the offset particle (f) Sliding variable

Figure 9(a)

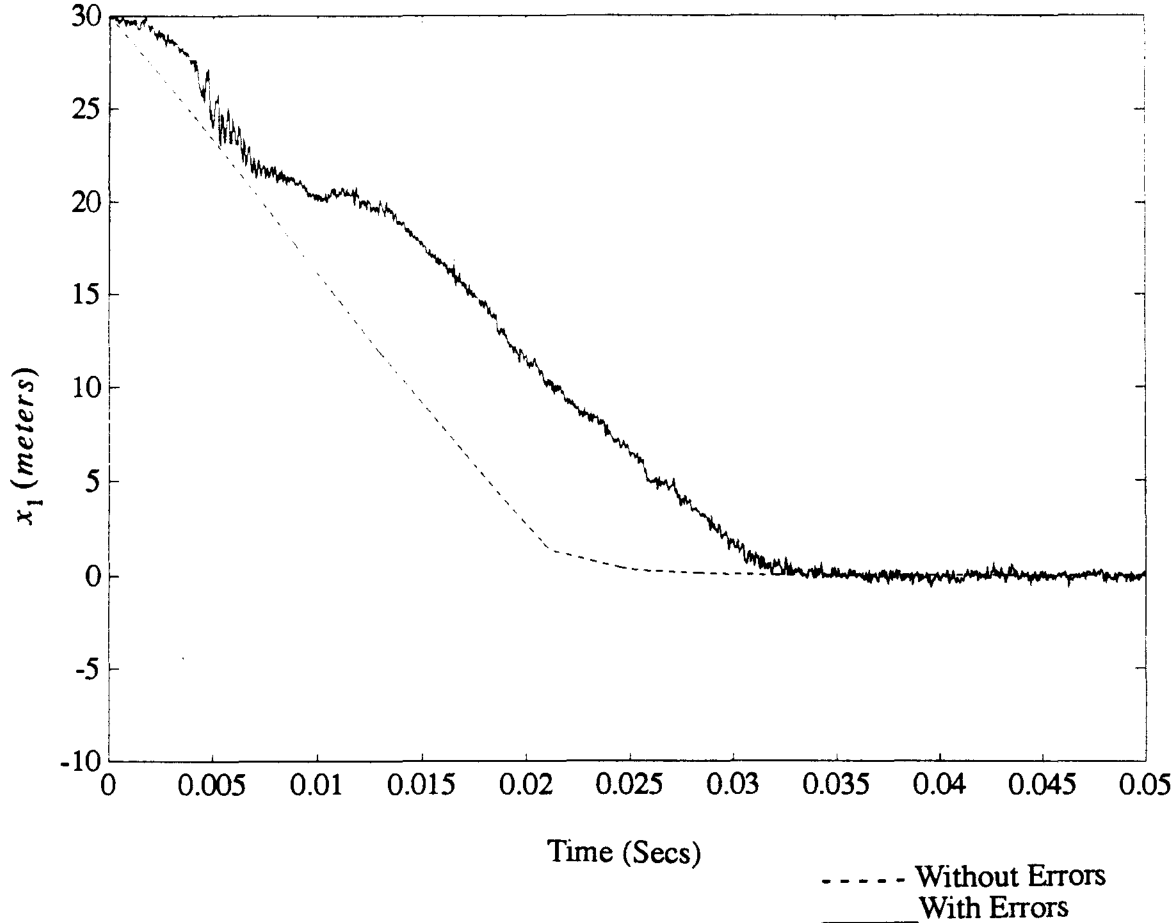

Figure 9(b)

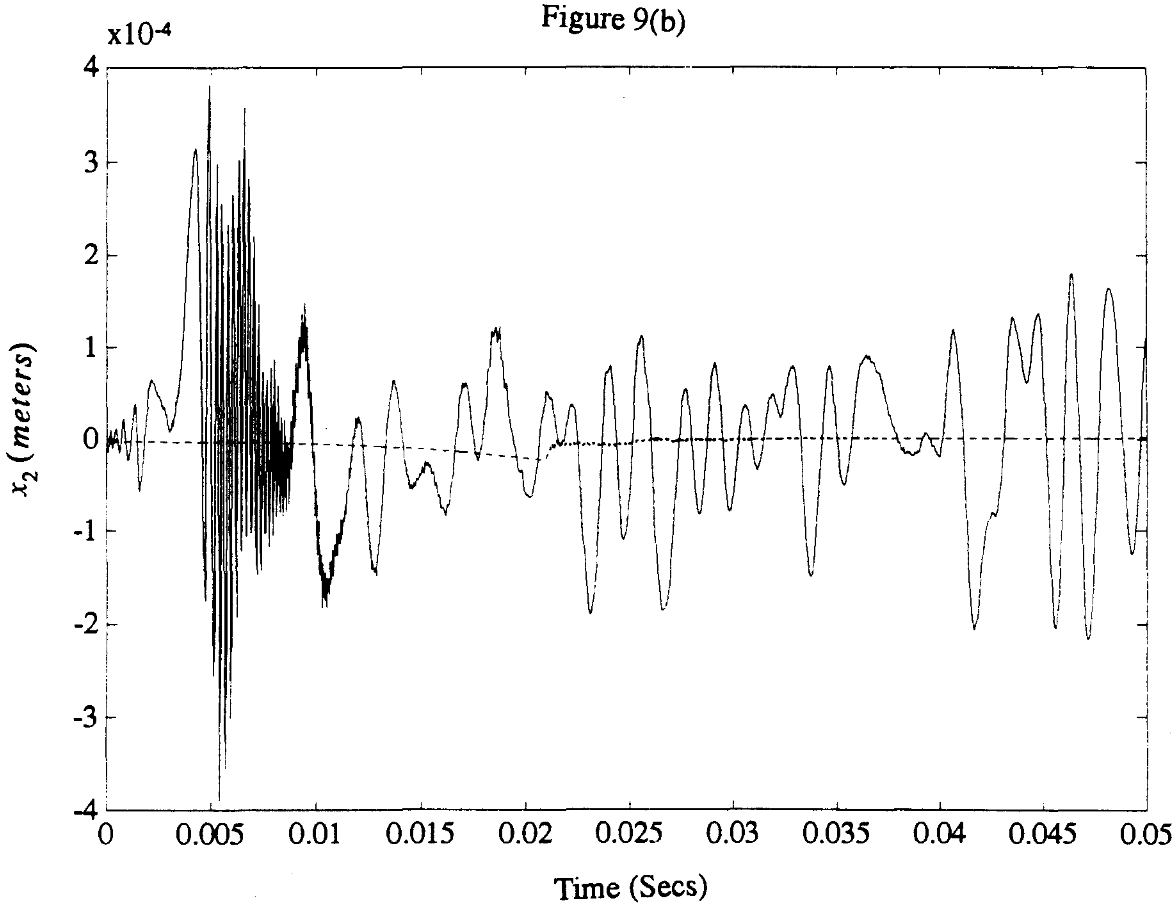

Figure 9(c)

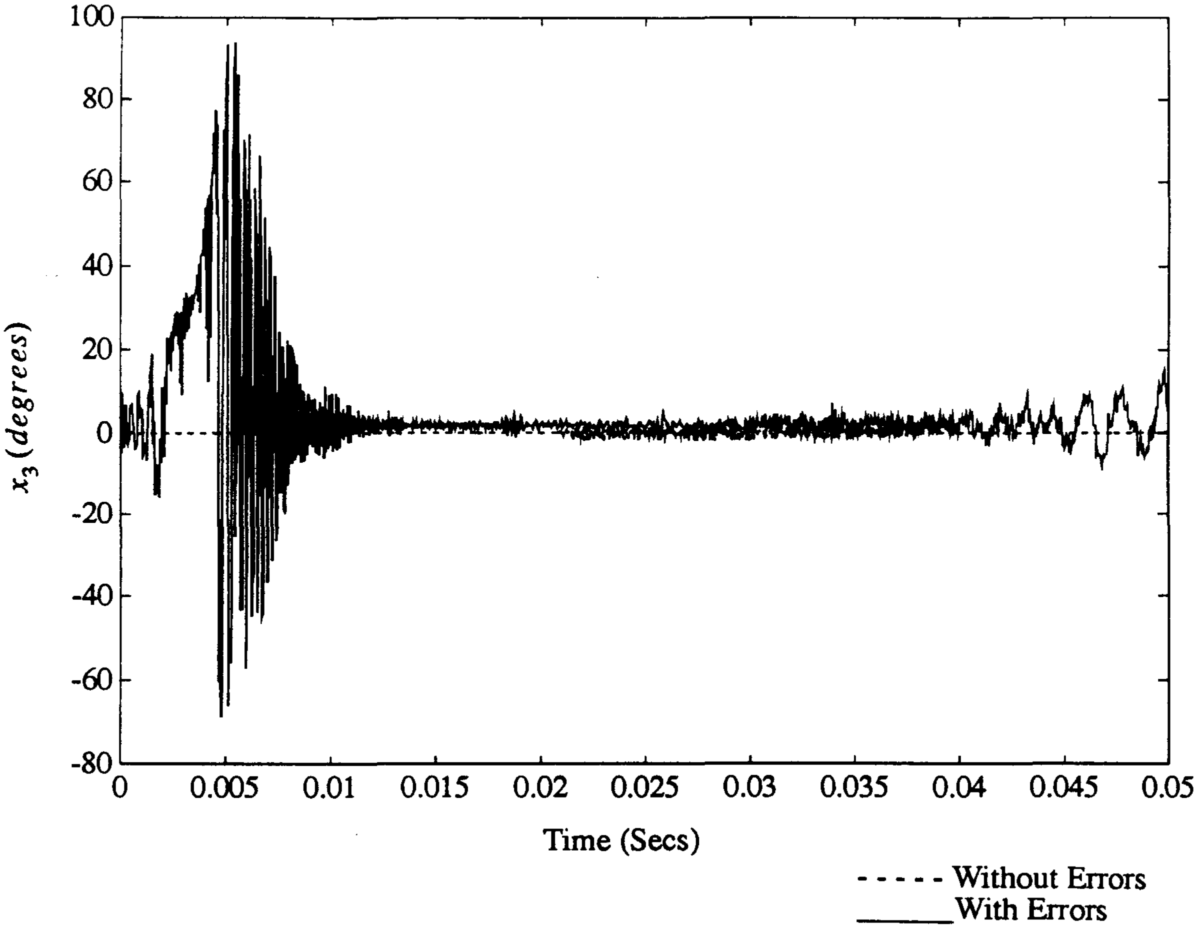

Figure 9(d)

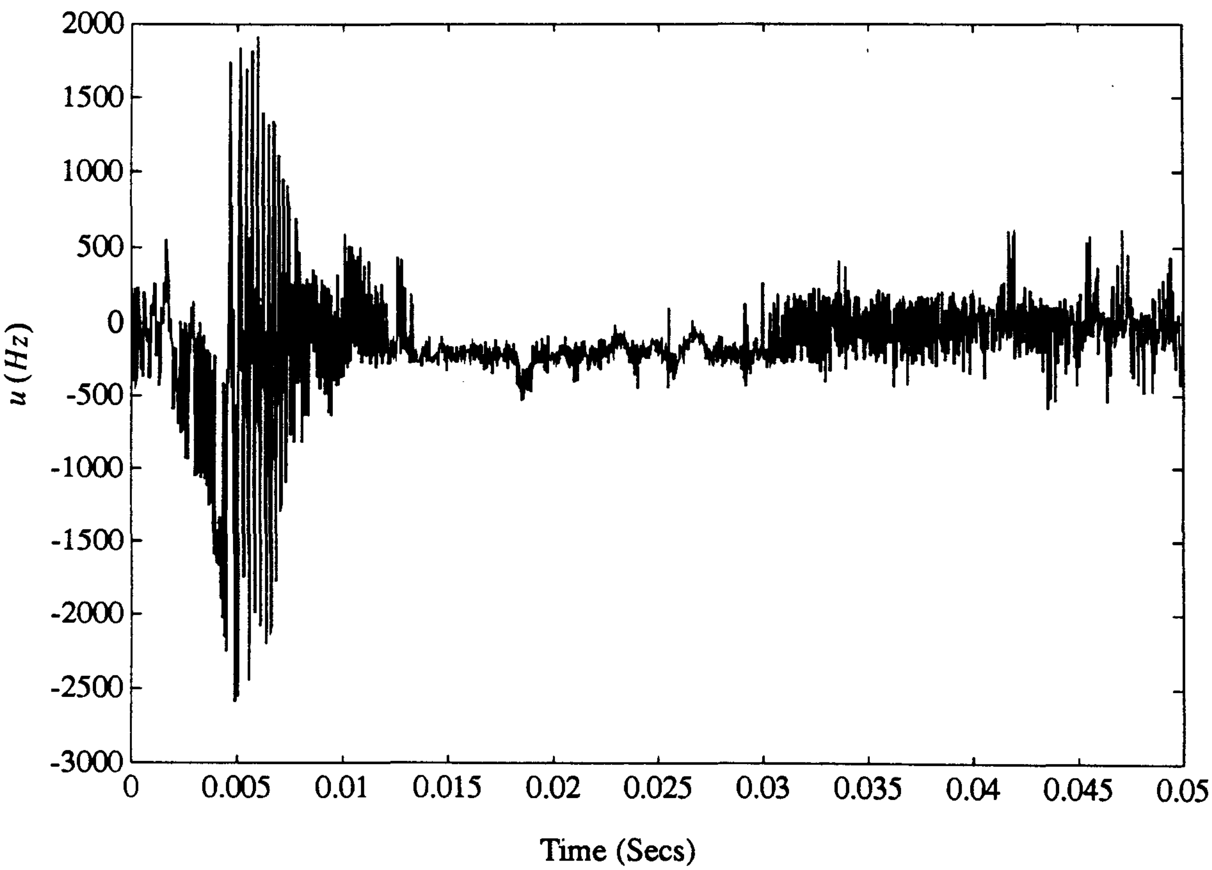

Figure 9(e)

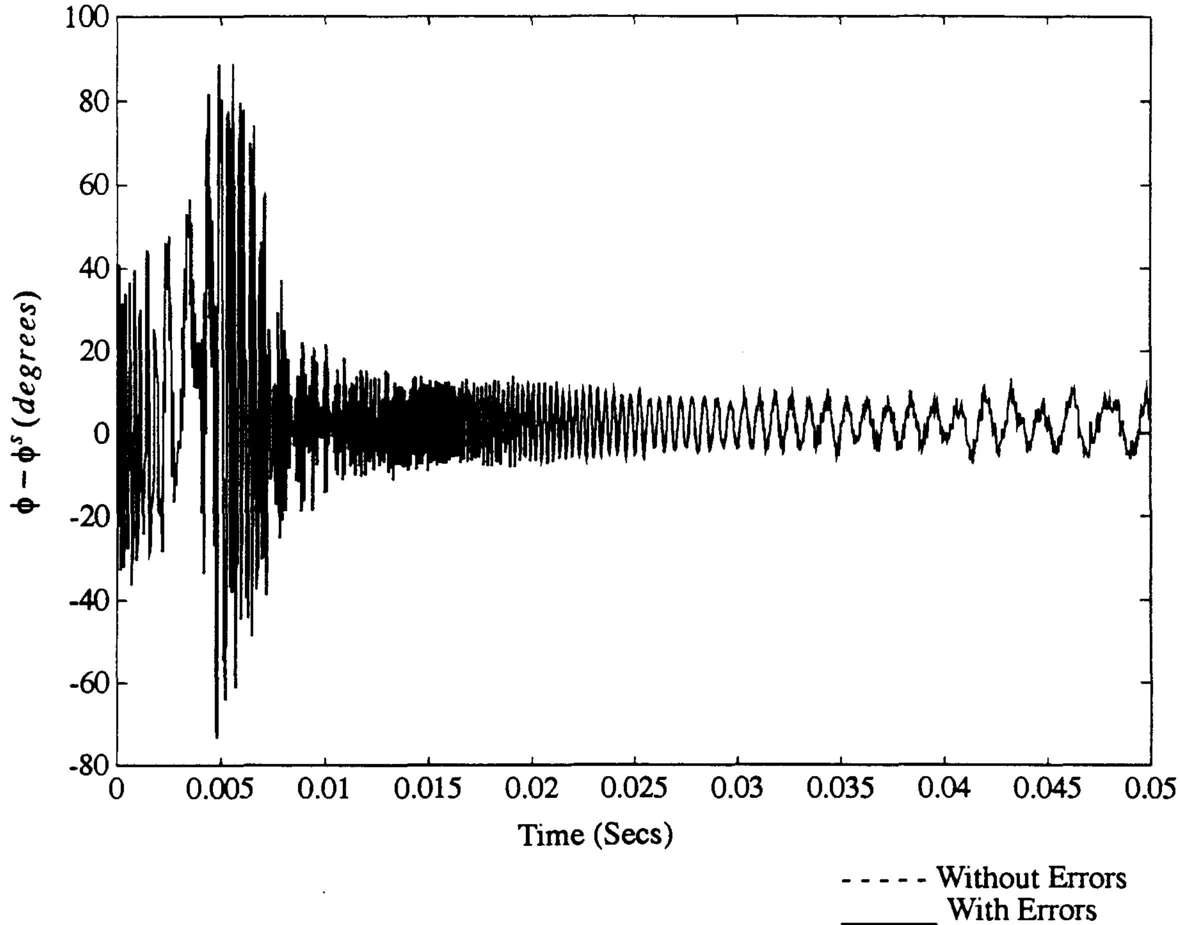

Figure 9(f)

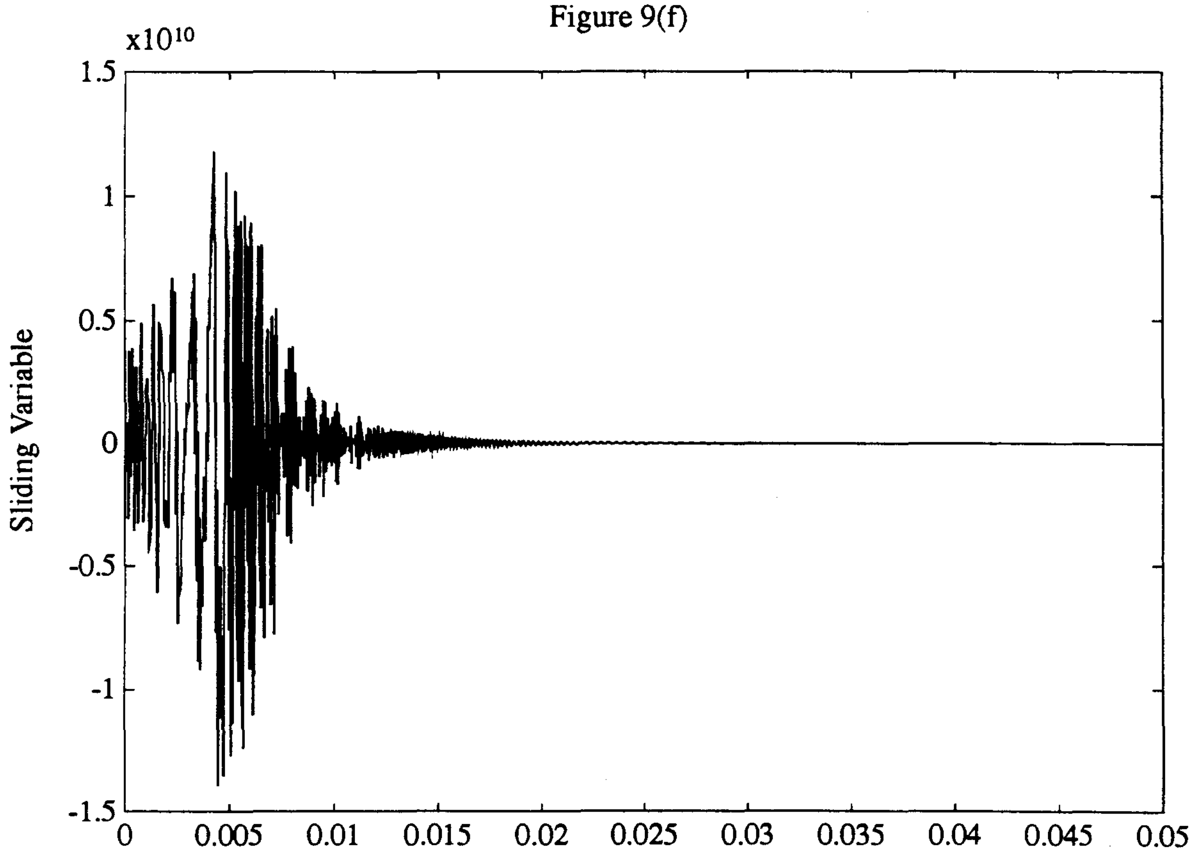

Figure 9. Simulation results for the modified sliding-mode controller
(a) Synchronization phase error (b) Radial orbit shift (c) Beam phase error
(d) Frequency shift (Control input) (e) Phase difference of the offset particle
(f) Sliding variable